Journal of Manufacturing Systems 57 (2020) 1–18

Contents lists available at ScienceDirect

Journal of Manufacturing Systems

journal homepage: www.elsevier.com/locate/jmansys

Application of sensing techniques and artificial intelligence-based methods to laser welding real-time monitoring: A critical review of recent literature

Wang Cai[a], JianZhuang Wang[a], Ping Jiang[a,*], LongChao Cao[a], GaoYang Mi[b], Qi Zhou[c]

[a] School of Mechanical Science and Engineering, Huazhong University of Science and Technology, Wuhan, 430074, China
[b] School of Materials Science and Engineering, Huazhong University of Science and Technology, Wuhan, 430074, China
[c] School of Aerospace Engineering, Huazhong University of Science and Technology, Wuhan, 430074, China

ARTICLE INFO

Keywords:
Laser welding
Real-time monitoring
Sensing techniques
Multi-sensor fusion technology
Artificial intelligence
Multi-monitoring objectives

ABSTRACT

Laser welding has been widely utilized in various industries. Effective real-time monitoring technologies are critical for improving welding efficiency and guaranteeing the quality of joint-products. In this paper, the research findings and progress in recent ten years for real-time monitoring of laser welding are critically reviewed. Firstly, different sensing techniques applied for welding quality monitoring are reviewed and discussed in detail. Then, the advanced technologies based on artificial intelligence are summarized which are exploited to realize varied objectives of monitoring such as process parameter optimization, weld seam tracking, weld defects classification, and process feedback control. Finally, the potential research problems and challenges based on real-time intelligent monitoring are discussed, such as intelligent multi-sensor signal acquisition platform, data depth fusion method and adaptive control technology. This fundamental work aims to review the research progress in laser welding monitoring and provide a basis for follow-on research.

1. Introduction

Laser welding is an efficient joining technique, owning to numerous advantages such as higher productivity, flexibility and effectiveness, deeper penetration of the weld seam, higher welding speeds, and power density [1–3]. That is why it obtains an increasingly widespread application in the automotive [4,5], shipbuilding [6], aerospace [7,8], micro-electronics [9,10], and other industries [11,12]. The welding quality can be disturbed by various factors during welding process, such as the internal defects of materials and the complex manufacturing environment [13,14]. The traditional off-line testing of welding quality can be costly in terms of time, material, and productivity. Therefore, several real-time welding quality monitoring solutions have been proposed to provide real-time information to control the welding process and welding quality [15,16]. During laser welding, keyhole [17], molten pool [18], plasma [19] and spatters [20] contain many kinds of welding signals, such as the acoustic signal, the optical signal, and the thermal signal, etc, which are closely related to the welding quality. Hence, a sensor based real-time monitoring system can obtain the welding signals effectively in the welding zone [21]. For example, a microphone [22] is used to collect the acoustic signal. Vision sensors like charge-coupled devices (CCD) [23], complementary metal-oxide semiconductors (CMOS) [18] and high-speed cameras [24] with special filters are applied to capture the images of the keyhole, molten pool, spatters and plasma. Spectrometers [25], and photodiodes [26] are utilized to collect the optical signals include visible light (VIS), infrared light (IR), and ultraviolet light (UV). The IR cameras [27], near-infrared (NIR) cameras [28], and pyrometers [29] can be exploited to gather the thermal signal. Complex monitoring system usually consists of the above-mentioned sensors and the welding signals will be more comprehensively collected. [30,31].

According to different monitoring objectives [32–34], there are many ways to reflect the quality of weld products. For instance, in order to achieve ideal penetration of weld seam, the extracted signal data will be used to optimize the welding process parameters [35] or to predict the penetration of the weld seam in real time [36]. So as to reduce the weld defects, online or offline monitoring of welding defects has been widely studied [37]. Seam tracking technology is an effective way to ensure that the center of the welding gap and the laser beam spot are consistent during the welding process [38]. Welding process feedback control technology can effectively avoid the influence of uncertain interfering factors on the welding quality [39]. Relying on reliable monitoring equipment [40,41] can obtain accurate signals, which is the basis of effective monitoring. Advanced data analysis methods can significantly improve the monitoring ability. In recent years, artificial intelligence (AI) [42,43], especially machine learning (ML) [44,45] has

* Corresponding author.
E-mail address: jiangping@hust.edu.cn (P. Jiang).

https://doi.org/10.1016/j.jmsy.2020.07.021
Received 14 June 2019; Received in revised form 9 May 2020; Accepted 27 July 2020
Available online 09 August 2020

Nomenclature

CCD	Charge-Coupled Device
OCT	Optical coherence tomography
CMOS	Complementary Metal Oxide Semiconductor
FEM	Finite Element Method
NIR	Near Infrared
BPNN	Back Propagation Neural Network
AI	Artificial Intelligence
PCA	Principal Component Analysis
ML	Machine Learning
RBFNN	Radial Basis Function Neural Network
DL	Deep Learning
GA	Genetic Algorithm
IR	Infrared
SVR	Support Vector Regression
NDI	Non-Destructive Inspection
PNN	Probabilistic Neural Network
EMAT	Electromagnetic Acoustic Transducer
KF	Kalman Filtering
LEU	Laser EMAT Ultrasonic
SVM	Support Vector Machine
UV	Ultraviolet
FVM	Finite Volume Method
VIS	Visible Light
PID	Proportional Integral Derivative
ICI	Inline Coherent Imaging
ANFIS	Adaptive Neuro-Fuzzy Inference System
MOI	Magneto Optical Imaging
CNN	Cellular Neural Networks

been gradually exploited in laser welding monitoring. Good results have been achieved in all aspects of welding monitoring [46], such as the depth mining of welding signal data, the prediction of weld morphology and the classification of welding defects [47]. So, the advanced monitoring equipment combined with effective AI-based methods has gained great achievements in laser welding real-time monitoring [48]. However, there are still some problems that hinder the application of real-time monitoring in industrial manufacturing. For example, some advanced monitoring equipment such as the X-ray imaging system is too expensive to apply in a factory and X-ray is also harmful to health. The Multi-sensor data fusion method is not intelligent enough, and the process of feature extraction, data mining and data fusion will cost a lot of time [49]. The application of deep learning (DL) [50] has just started in recent years, and how to make full use of the merits of data mining and self-renewal learning abilities are the key issues to shorten the data processing time and improve the monitoring accuracy.

In this paper, an overview of laser welding real-time monitoring was arranged in detail. Fig. 1 shows the content structure of this paper and the review content can be divided into two important parts. In the first part (including Section 2 and Section 3), it begins with a detailed introduction about the laser welding monitoring process. Then, some commonly used monitoring sensors and methods, some novel monitoring techniques, and the multi-sensor fusion method were sorted and summarized respectively. In the second part (including Section 4), numerous AI-based methods were reviewed according to different monitoring objectives such as seam features prediction, defects classification, adaptive control, etc. Finally, the potential future research work and challenges about the intelligent monitoring of the welding process were discussed. This paper aims to provide a basis for follow-on research by reviewing the research trends in the past ten years.

The paper is organized as follows. For better understanding the real-time monitoring process, the laser welding process is introduced in Section 2. Next, sensors and methods in laser welding monitoring are discussed in Section 3. In Section 4, methods used for achieving different objectives are talked over. Finally, highlights in the potential research issues are given in Section 5 and conclude the paper in Section 6.

2. Understanding the laser welding monitoring process

Laser welding real-time monitoring can effectively reduce the negative impact of various uncertain factors on the welding quality [51–53]. The monitoring process can be divided into three different parts: the pre-processing scanning, the in-process monitoring, and the post-process diagnosing [1,54]. The different stages of welding monitoring are shown in Fig. 2. The pre-process scanning [28] mainly focuses on the seam tracking problem, scanning the joint gap between workpieces to ensure that the laser beam spot focuses on the gap center to obtain reliable joints. The in-process monitoring [55] pays close attention to the real-time monitoring of welding characteristics in the welding zone such as keyhole, molten pool, plasma and spatters, etc. by using various equipment. By analyzing the dynamic changes of these characteristics, the quality of the weld seam can be predicted and adjusted by effective AI-based methods. The post-process diagnosing [37]

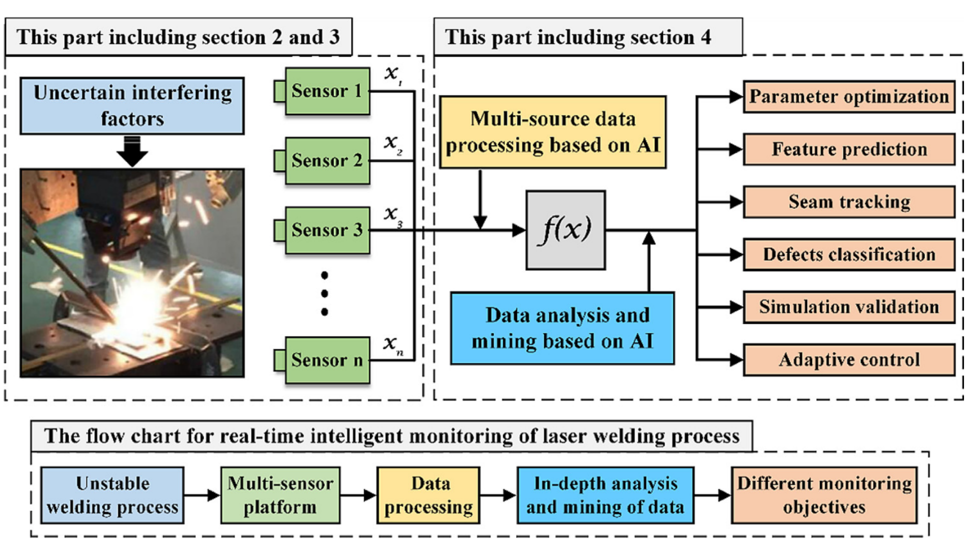

Fig. 1. The review structure of this paper and the flow chart of the monitoring process of laser welding.

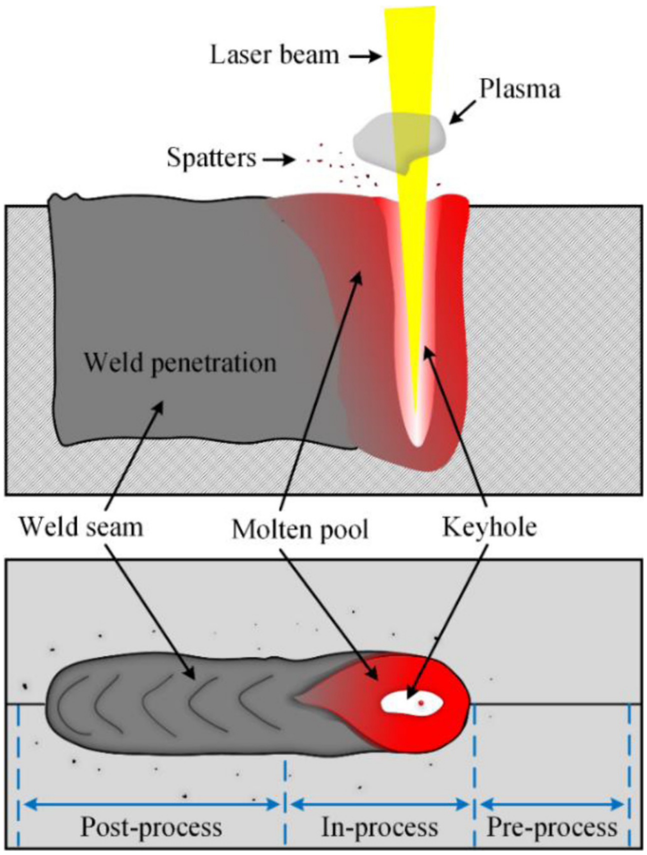

Fig. 2. The schematic of laser welding and the definition of the different monitoring stages.

concerns the problem of the defects diagnosis. The pore, crack, spatters, surface collapse, underfill, etc. are the common defects of weld products which are the critical indicators in the quality evaluation of weld seam [56]. Depending on the defect diagnosis technology, the weld defects can be found in time to assess the quality of the weld seam, which is beneficial to improve the product qualification rate [57]. Table 1 mainly summarizes the monitoring objectives, monitoring signals and monitoring technologies in different stages of welding monitoring. To find better monitoring techniques, some researchers studied these three processes separately, while others hoped to develop a system to monitor these three processes at the same time. Katayama et al. [58–60], Zhang's team [61,62], Webster et al. [63–65], and the group lead by Gao [24,49,66,67], etc. focus on the various welding signals in the welding area. Real-time monitoring of these signals provides reference data for real-time adjustment of the welding process. Dorsch et al. [68] exploited a triple-sensor system to monitor the pre-, in- and post-process simultaneously. Fig. 3 shows the structure of this system and the monitoring results during welding a powertrain gear. A detailed review of real-time monitoring during the pre-, in- and post-process are exhibited in Section 3 and Section 4.

3. Different sensing techniques

In this section, some commonly used sensors and novel monitoring methods, and the most widely used multiple sensor fusion monitoring technology are discussed in detail for a better understanding of the collection process of the welding signals. The detailed classification of monitoring sensors and techniques are shown in Fig. 4. At the end of this section, according to different monitoring technologies, sensors and monitoring welding phenomena, the references are classified and shown in Table 2.

3.1. Basic sensors in monitoring

3.1.1. Acoustic emission signal

When the plasma is ejected from the keyhole, the pressure fluctuations therein bring about the acoustic signal, which can be non-contact measured by using a microphone or resonant sensor [57]. Acoustic monitoring methods obtain great attention due to the affordable cost and simplicity of operation [69,70]. Huang et al. [71] investigated the relationship between the penetration of the weld seam and the acoustic signal. The acoustic signatures, such as sound pressure deviation and band power, are defined and extracted. Then, these signatures are used to characterize the weld penetration by applying neural network algorithm and multiple regression analysis methods. The results showed that the algorithms could effectively distinguish full penetration from partial penetration. However, the acoustic signal is susceptible to environmental noise which obstructs the forthputting of the acoustic signal monitoring. In [72], by using two noise reduction methods to the acquired acoustic signals, the background noise signals have been effectively reduced. Luo et al. [73] created a plane microphone array system, which is composed of eight microphones to capture the acoustic signal. Results revealed that this system reduced the surrounding noise. Lv et al. [22] designed an automatic measure and control system to control arc length in real-time by analyzing the audio data. The linear fitting model was implemented based on the linear relationship between the arc sound and arc length, which can be used to predict the surface height of the molten pool, and good prediction results were achieved. Ao et al. [74] built a two-dimensional simulation model to reveal the acoustic signal features which are caused by the vapor flow during the welding process. The simulation results indicated that the velocity of the vapor flow in the center of the keyhole is higher than the vicinity of the keyhole. The maximum velocity of the vapor flow inside the keyhole could reach 280 m/s. The experimental results were consistent with the simulation results, which proved the effectiveness of the simulation model.

The ultrasonic signal generated during the laser welding process has great significance in non-destructive inspecting (NDI) the internal defects of the weld seam [75–77]. Passini et al. [78] investigated the ultrasonic phased array inspection technology to detect the welding defects in thin aluminum sheets. The detection results of this inspection method on the quality of the weld seams were compared to the X-ray radiography and metallographic inspections. Results showed that this method was able to identify the presence of grouped porosity. The electromagnetic acoustic transducer (EMAT) is a new technology emerging in the field of NDI that uses an electromagnetic coupling to excite and receive the ultrasonic waves. The EMAT method is more accurate than traditional ultrasonic inspection technology. The Laser EMAT ultrasonic (LEU) technique can be used to measure the

Table 1
Monitoring objectives, monitoring signal and monitoring technology in different monitoring stages.

Three quality monitoring stages	Monitoring objectives	Monitoring Signal	Monitoring technology
Pre-process	Seam tracking Gap measuring	Optical signal	Machine vision Laser triangulation
In-process	Welding stability Defects monitoring Molten pool and keyhole geometry Feedback control Feature prediction	Acoustic signal Optical signal Electrical signal Thermal signal	See Fig.4
Post-process	Defects classification Weld geometry	Optical signal Acoustic emission	Machine vision Nondestructive inspection Metallographic test Laser triangulation

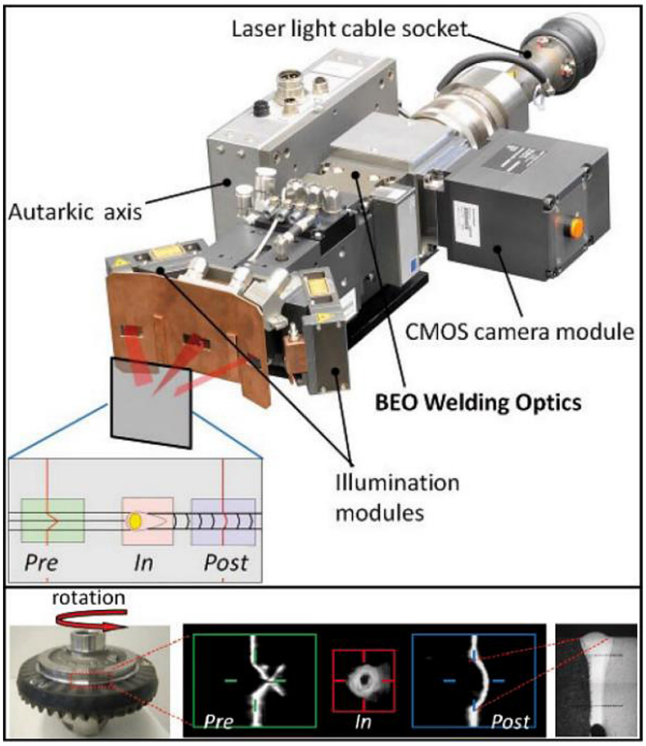

Fig. 3. The pre-, in- and post-process monitoring system and the monitoring results of powertrain gear [68].

penetration depths of the weld seam. Yang et al. [48] investigated the transmission coefficients of the Lamb waves which emerge in the LEU signals according to different penetration depths. The transmission coefficients and the energy of LEU signals were used to accurately predict the penetration depths of the weld seam by establishing an artificial neural network model. Due to the different time that the ultrasonic waves pass through the molten pool, the solid phase and the solid phase near the molten pool, Mizota et al. [79] exploited an ultrasonic phased array system to measure the depth of molten pool by calculating the time of the system received. Fig. 5 is the detailed schematic diagram of this inspection method.

3.1.2. Optical signal

Optical signal monitoring is mainly composed of optical radiation monitoring [80,81] and optical vision monitoring [82,83]. Optical radiation signal mainly comes from the laser beam and the welding area. The molten pool, spatters and plasma, etc. all emit strong optical radiation [84]. For example, the ultraviolet (UV) and visible light (VIS) radiation come from the atomic transitions and the bremsstrahlung within the plasma, and the IR radiation is emitted from both the hot plasma and the molten pool. In [85], the optical radiation signals can be divided into two categories according to different wavelength. The first category is UV and VIS radiation, and the wavelength is from 0.3 μm to 0.7 μm. Another type is IR radiation between 1.1 μm and 1.6 μm. The spectrometer and photodiode sensor can be applied to collect the optical radiation signals. Eriksson et al. [86] utilized three photodiode sensors to obtain independent information about the thermal (the T signal) condition of the molten pool, the radiation from plume (the P signal) and the reflected (the R signal) radiation of laser beam. The wavelength of the R signal is about 1.0 μm and detailed optical radiation bands are shown in Fig. 6 (a), and Fig. 6 (b) is the schematic of this monitoring system. In [87–89], Sibillano's team researched the optical radiation which emits from the plasma plume. A spectroscopic sensor-based system was exploited to collect this signal, and this monitoring system was available on the market. They also studied the correlation between the temperature of the plasma electron and the penetration depth of the weld seam by using the spectrometer system which equipped with a CCD detector array. Zaeh et al. [90] provided a novel insight into the origin of the radiation emissions. The results indicated that the alloying elements influenced the mechanical properties of the weld joint. Combining with the published results presented in [91,92], an in-situ melt identification system was established, which was able to measure the concentrations and concentration variations of different alloying elements in the weld seam. By doing a lot of experiments, Mrna et al. [93] proved the correlation between the penetration depth and the frequency features of the light intensity oscillations which can be used as a basis for exploiting a universal method to optimize and control the welding process. Bono et al. [94] utilized an optical-based monitoring approach to find the relationship between the photodiode signals with different weld characteristics and imperfections. They also investigated a novel monitoring approach which based on laser interferometry. This approach can measure the depth of the keyhole in real-time. The effectiveness of both approaches had been confirmed by experiments.

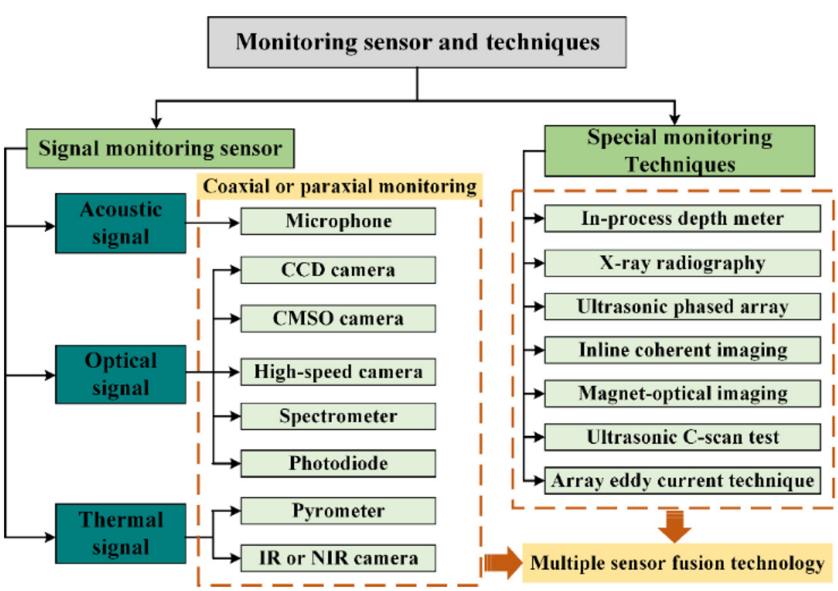

Fig. 4. The classification of sensor and techniques.

Table 2
Paper's classification based on the different sensors, monitoring technology and welding phenomena.

	Traditional monitoring methods (Single sensor)						Novel monitoring technology	Multi-sensor fusion
Sensor or method	Microphone	Vision camera	Spectrometer	Photodiode	IR or NIR camera	pyrometer	X-ray, ICI, MOI, etc.	Multi-sensor
Monitoring phenomena	Vapor plume Workpiece	Plasma Molten pool Keyhole Spatters Welding gap	Spectrum of plasma	Plasma Thermal radiation Reflected laser beam	Thermal field	Temperature of plasma Temperature of molten pool	Keyhole depth Welding gap Weld seam geometry Inner defects	Welding zone Welding gap Thermal field Spectrum of plasma Keyhole depth Weld seam geometry
reference	21 − 22, 55, 66 − 76	17 − 18, 23 − 24, 39, 42, 48, 60, 93 − 96,98 − 109, 114, 136 − 137	25, 77 − 78,84 − 87,120, 133 − 134	19, 26, 81,90 − 91	27 − 28, 36, 40, 44, 119, 128 − 132, 135	29, 122 − 127	34, 38, 41, 46, 61 − 64, 80,139 − 142,144 − 151, 153 − 165	16, 30 − 31, 37, 45, 47, 51, 53, 56 − 58, 65, 79, 83, 92, 97, 101, 110 − 113, 115 − 117,138, 166 − 184
Limitations	Sensitive to the noise of environment	Auxiliary equipment required and images need further processing	Monitoring only plasma behavior	Inefficient in identifying microdefects	Low sampling and high cost	Low sampling and No defect information	High cost and Limited use environment	High cost, Complex signal analysis, Inconsistent signal dimensions

Optical vision monitoring method is widely used at present [95–98], due to a large amount of reliable data can be obtained by this method. Morphological characteristics of the keyhole, molten pool, spatters and plasma plume, etc [99–101]. are constantly changing during the laser welding process. These dynamic signals produced during the welding process are closely related to the fluctuation of the welding quality. Gao et al. [102] quantificationally characterized the relationship between the morphology features of the molten pool and the stability of the laser welding process, which provides a basic understanding of the real-time monitoring of molten pool behavior. Zhang et al. [103] analyzed the time and frequency domain characteristics of the keyhole and the plasma plume. Results offered a basis for the on-line inspection of laser welding of tailor rolled material. Kim et al. [104] investigated the dynamic behaviors of the keyhole by using the image processing method under different welding conditions. Tenner et al. [105] measured the velocity and direction of the fluid flow inside the keyhole with very high precision by attaching a glass plate. Findings showed that the fluid flow related to the laser power, feed rate and welding gap. The CCD camera [106], high-speed camera [107] and CMSO camera [108] are commonly used sensors for capturing images like plasma or molten pool etc. during laser welding, and Fig. 7 shows the different arrangements of sensors in visual monitoring. In order to reduce the strong optical radiation, the multiple filters [100,109] and the auxiliary light source [110] illumination system are applied. Luo et al. [18] presented a useful technique to obtain the edge of the molten pool. The CMOS camera was used to capture the dynamic images of the molten pool, which was illuminated by using an auxiliary green laser. The validation experiment proved the effectiveness of this monitoring method. Zhang et al. [111] applied a CCD camera to capture the dynamic images of the molten pool and keyhole. In [112], fifteen features of the vapor plume and spatters were defined and extracted to evaluate the quality of the weld seam. However, a signal camera sensor is limited in data acquisition due to spatial constraints. More and more researchers choose multiple camera sensors [113] to observe the welding zone. By monitoring from different angles, comprehensive information can be obtained for future research. Wang et al. [114] applied two high-speed cameras to photograph the instantaneous visual phenomena such as the metallic vapor and the spatters, and the bottom surface of the keyhole were monitored at the same time for evaluating the keyhole status. In [115], the molten pool upper surface and lower surface were observed synchronously by using two CCD cameras. Results showed that the upper surface was shorter and more stable than the lower surface. You et al. [116] used two high-speed cameras to collect the images of spatters in the NIR, and the UV/VIS waveband together. It was found that the UV/VIS waveband was more appropriate for monitoring the spatters. Chen et al. [117] established a monitoring system combined with four CCD cameras. The monitoring effects were studied in both static and dynamic cases. However, the increase in the number of cameras will lead to an increase in costs. Fan et al. [118] designed a three-optical-route visual sensor system to monitor the molten pool from three directions at the same time. This system reduced the cost and achieved good results. Liu et al. [119] acquired the monitoring pictures from the underside of the welding work-piece when the keyhole penetrated fully. In [120], a high-speed observation system of visible and infrared radiation was established to monitor the molten pool, the solid-liquid interface and the temperature profile.

3.1.3. Thermal signal

Laser welding is a thermal manufacturing process, the material is melted by the laser beam. The thermal radiation signal is significantly strong in the welding zone, especially in the keyhole [122], the molten pool which formed by the molten metal [123] and the high-temperature metallic vapor [124]. In the ideal conditions, the spectral radiance $L_{\lambda S}$ of a black body can be described by the Planck's law [125] as below,

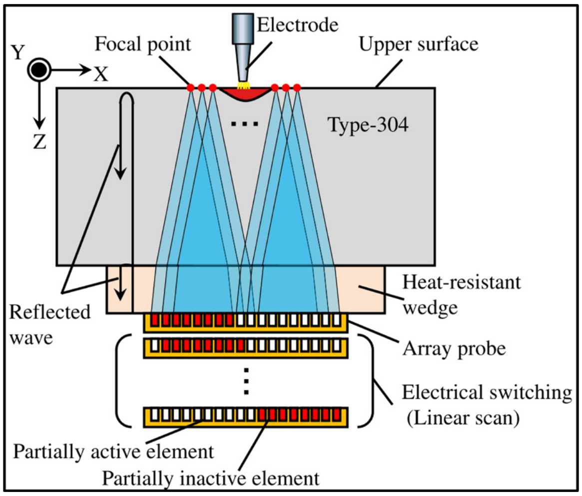

Fig. 5. Schematic image of molten pool depth measurement using an ultrasonic phased array system [79].

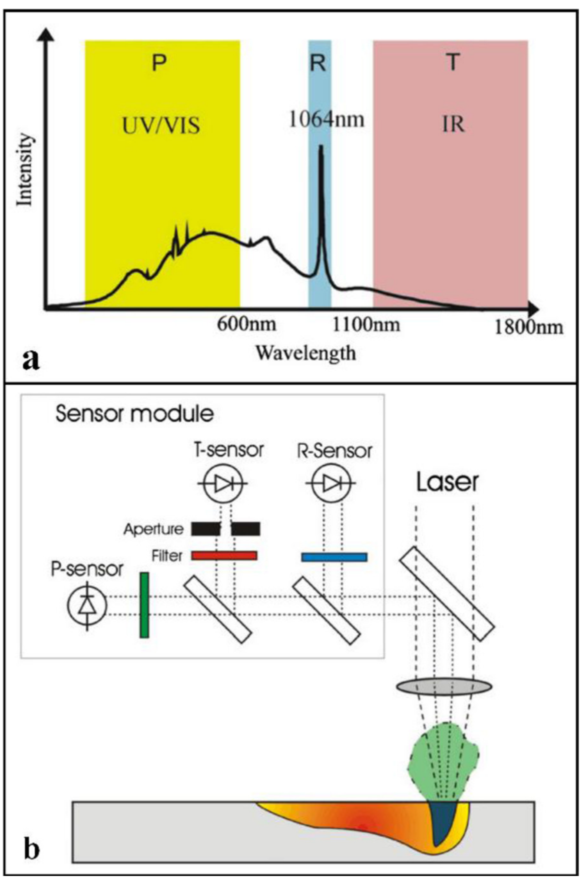

Fig. 6. The monitoring spectral range and the schematic diagram of this monitoring method [86].

$$L_{\lambda S} = \frac{C_1}{\pi}\cdot\frac{1}{\lambda^5}\cdot\frac{1}{\exp\left(\frac{C_2}{\lambda\cdot T}\right)-1}Wm^{-3}\cdot sr^{-1} \tag{1}$$

where λ is the wavelength. T presents the absolute temperature. C_1 and C_2 are constants. Fig. 8 (a) shows the black body emission spectra for various temperatures. The overall emitted radiation depends on the temperature, which is very high in the welding zone, and the thermal radiation is very strong. Pyrometer [126,127] and IR camera [128] are commonly used sensors to obtain the thermal signal. The merit of the pyrometer is that it is cheaper and easy to assemble. Yamazaki et al. [129] used an IR two-color pyrometry to measure the temperature of the metal droplet during metal active gas arc (MAG) welding. The temperature distribution of the droplet surface was studied based on the IR range. Kohler at al [130]. combined ratio pyrometry with two-dimensional-resolved measurement to acquire the thermal signal. It is proved that the emissivity and the attenuation of thermal radiation were independent of two-dimensional temperature information. This novel method could be used to measure the diameter of the molten pool, the latent heat, and validate the simulation based on FEM. The pyrometer sensor can also be used in harsh environments, but limited by the sampling frequency. Doubenskaia et al. [131] researched the sampling frequency when detecting the welding defects. The advantage of IR camera [132] is that it can reflect the temperature distribution of the welding zone more comprehensively. In [27], an IR thermography was used to collect the surface temperature information. By comparing the obtained data with the numerical simulation outcome, the result showed that the IR sensor could accurately monitor the temperature of the welding zone. In [133,134], the real-time IR images of the molten pool were applied to estimate the width and the depth of the weld seam. The prediction results were in good agreement with the actual measurement results. Weberpals et al. [135] investigated the temperature distribution and geometrical structure of the welding zone by analyzing the emitted thermal radiation. This novel monitoring approach could be used to determine the inclination of the keyhole. Chen et al. [136] applied a high-speed IR video camera to obtain the IR images of the molten pool and their adjacent areas. This high-speed imaging system can accurately extract the shape characteristics of the molten pool, which can be used to reflect the information of the weld quality. Results showed that these characteristics of the molten pool could effectively reflect the stability of the welding process. Plasma plume also contains the information about the thermal signal. Chmekuckova et al. [137] calculated the relative intensities of couples metal ion emission lines in the plasma plume at actual welding conditions to establish a numerical simulation model of the cross-section of the welding zone to display the temperature distribution when the laser power is increasing. Chen et al. [138] exploited an optical multi-channel analyzer which can simultaneously acquire the spectral signals from multiple independent points. The obtained spectral signals were processed by the Abel inversion method, and the temperature fields of the keyhole and the plasma plume were established.

3.2. Monitoring methods

3.2.1. Traditional monitoring methods

The traditional monitoring methods are applied to some common sensors to monitor the welding process in coaxial or paraxial [17,140]. Both approaches have their own advantages and deficiencies. Coaxial monitoring [108] method can monitor from directly above the welding zone by installing the spectroscope in the laser propagation path. The obtained optical and thermal signals are stable and less disturbed. However, the installation of the monitoring sensor is complex, and this method is not flexible enough. The reflected laser radiation and plasma may also affect the observation of the keyhole and molten pool. The merit of paraxial monitoring [141] is that the monitoring distance and angle between the sensor and the welding zone are easy to adjust. By repeated calibration and comparison, the best monitoring location can be found and recorded. The optical and thermal signals can be monitored simultaneously coaxially and paraxially [142]. Microphone for acoustic signal acquisition [72] and pyrometer [131] for thermal signal detection are usually paraxial assemble. Multi-sensor fusion technology and some novel monitoring methods are usually based on these traditional monitoring methods, which will be discussed in the next two parts.

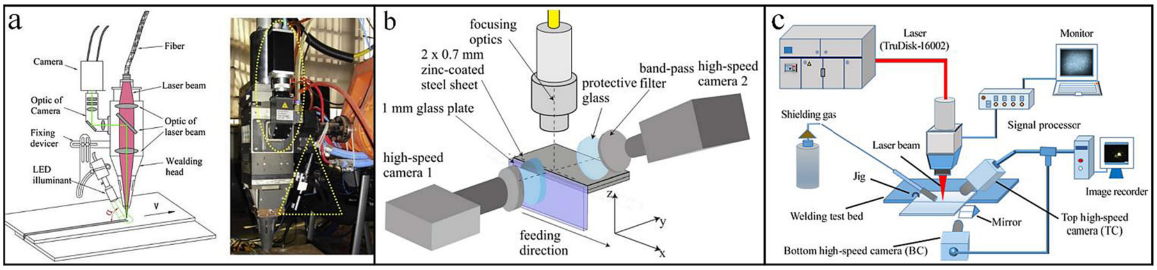

Fig. 7. Different vision monitoring system. (a) Coaxial monitoring system with an auxiliary illuminant [100]. (b) The melt velocity measuring system with two high-speed cameras [105]. (c) The top surface and bottom surface are simultaneously observing system [121].

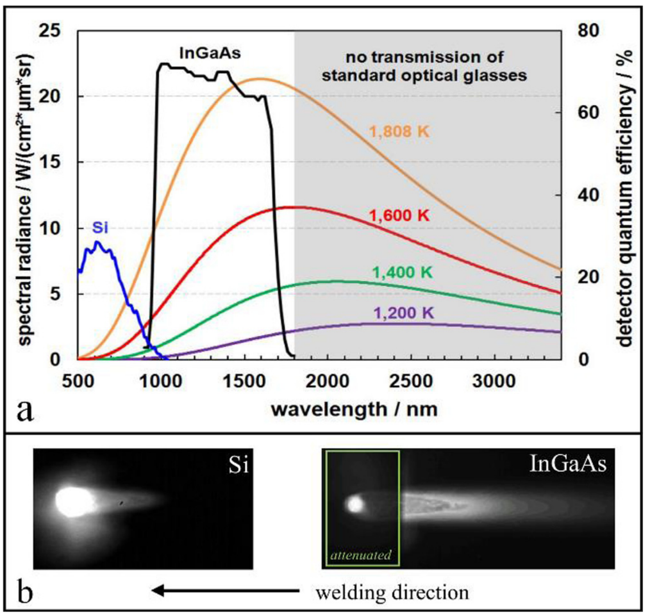

Fig. 8. NIR-camera-based online diagnostics [139]. (a) Black body emission spectra based on Planck's law for different temperatures in comparison to Si and InGaAs detector sensitivity. (b) Comparison of images of the welding zone and its surrounding as taken with a Si- (left) or an InGaAs- (right) camera.

3.2.2. Novel monitoring methods

Some welding features are difficult to obtain during the welding process, but they are closely related to the welding quality. For example, the depth of the keyhole [143] is directly related to the penetration depth of the weld seam [144]. If the keyhole depth can be obtained in real-time, it will be very helpful to judge the weld penetration. Some novel monitoring methods, namely X-ray imaging technique [145], inline coherent imaging (ICI) [146], magneto optical imaging (MOI) [34], have been proposed and achieved excellent results. The X-ray is an efficient NDI technology which has been applied in many filed [147–149], i.e. medical science [150], laser welding real-time monitoring [151] and soil science [152], etc. In-situ X-ray videography makes it possible to obtain time and space resolved information about the keyhole geometry during the welding process [153]. The X-ray technique can also be used to diagnose the inner defects of the weld seam with the high spatial and high temporal resolution [154]. Yan et al. [155] investigated the microstructure and mechanical properties of the weld seam by using an X-ray diffraction system. The obtained phase compositions were observed by the microscopy to study the microstructure characters of joints. The X-ray diffraction system was also used to measure the residual stress distribution in the weld seam [156]. Norris et al. [157] researched the formation process of pores in milli-scale keyhole mode welding by analyzing the process parameters, including the laser power, the welding speed, and the size of the laser beam. The X-ray radiography was used to obtain the porosity characteristics, and the results were contrasted to the metallographic analysis. The optical coherence tomography (OCT) is an innovative sensor 3D measuring technology for automated laser welding. It provides an industrial solution to inspect the keyhole depth in real-time during the welding process [158]. Ackermann et al. [159] exploited an inline monitoring device based on the Fourier-domain OCT to extract the tomographical geometrical measurement data during the weld seam forming process. The ICI monitoring technology adapts the idea of OCT to laser processing metrology field [160]. The schematic diagram of ICI system is shown in Fig. 9 (a), and the ICI system is composed of a fiber-optic Michelson interferometer [161]. The imaging beam is delivered coaxially with the laser beam so that the imaging beam can reach the bottom of the keyhole to measure the depth. Fig. 9 (b) is the fitting graph of the profile of weld penetration and the measured keyhole depth (green dots). It can be seen that the curve composed of green dots is consistent with the weld penetration. This novel technique can obtain the required precision of data and guarantee the flexibility, stability and the traceability of monitoring process, which has been widely applied in the welding process monitoring [162–164], the break-through detection [160] and the forward-viewing tissue ablation observing [165], etc. Gao et al. [166] monitored the micro gap welding (gap width < 0.05 mm) process by using MOI technique. The MOI method is based on the magnetic induction principle and the Faraday rotation effect [167]. In the experiment, a magnetic excitation device was used to

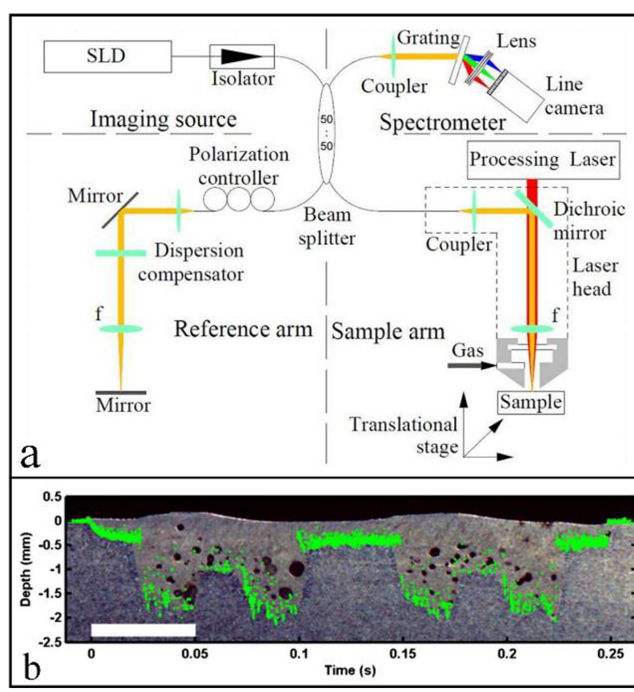

Fig. 9. (a) the schematic diagram of the ICI system, (b) the ICI measured depths (green dots). [146]. (For interpretation of the references to colour in this figure legend, the reader is referred to the web version of this article.)

magnetize the workpiece, and a magneto-optical sensor was applied to detect the magnetic field distribution for further research [168]. In [169], the MOI method was compared with the traditional methods through actual physical experiments. Results indicate that the microstructure of the weld joint could be inspected by MOI method without the metallographic preparation process. Furthermore, Todorov et al. [170] investigated the array eddy current technique to inspect the missed seam defect and lack of penetration by scanning the top and bottom surfaces of the weld seam and achieved good results.

3.2.3. Multi-sensor fusion technology

The laser welding process is very complicated where the melt and vapor flow, heat transfer, phase change, the laser beam interaction with the plasma, and the multiple reflections of laser beam coincide. Many of the above welding signals are related to the welding quality, with only one type of monitoring sensor or method [171]. The welding situation can not reflect fully. Consequently, the proposed multi-sensor fusion technology can monitor the welding process more effectively and comprehensively [172,173]. Because this monitoring method can make full use of the advantages of various signal sensors. The vision sensors can supply rich information about the welding zone and have become the core sensor of multi-sensor fusion technology. The established monitoring system usually includes one or more vision sensors [174,175]. For example, the optical sensor combined with the vision sensor [176,177], The X-ray system combined with the high-speed camera [178,179], the sound sensor assembled with the vision sensor [180] and other combination methods [181,182]. Chen et al. [183] applied the arc sensor and the CCD camera to obtain the electronic signal and the molten pool images at the same time. This method can extract multi-features to forecast the backside width of the molten pool more accurately. In [184], a sound sensor was added, and these three sensors were used to collect the weld current, voltage, the molten pool images, and the sound signal simultaneously. Multi-signal fusion method is critical in the multi-sensor system. In [185], the weighted mean method was used to fuse the voltage and sound features to predict the dynamic changes of arc length. Zhang et al. [16] proposed a feature level data fusion method to evaluate the quality of the weld seam in real-time. The obtained signals were processed and analyzed in the time and frequency domain, and the multiple feature parameters were successively extracted. Boley et al. [186] researched the 3D shape of the molten pool and the capillary reconstruction method during the welding process. Three different diagnostic methods, including the X-ray system, the optical videography sensor, and the metallographic cross-sections observation, were combined to gain the 3D form data of the welding zone. Harooni et al. [187] measured the electron temperature of the detected spectral signals by using the Boltzmann plot method and investigated its correlation with the pore formation. You et al. [188] applied two photodiodes and two visual sensors to monitor the laser welding process at the same time. The obtained signals were analyzed by applying the signal processing method and the image processing method, and five welding features were extracted and fused to described the welding process more precisely. Fig. 10 shows a schematic diagram of the sensor arrangement for a typical multi-sensor fusion technology. The used sensing devices include two photodiodes, a spectrometer, two visual cameras, and an X-ray sensing system. Results indicated that this monitoring system could collect accurate and effective welding signals to analyze and model the laser welding process more comprehensively.

4. The methods for realizing varied monitoring objectives

A complete monitoring process needs to collect and analyze the signal data generated during the welding process. In Section 3, different sensors and monitoring methods [190,191] are reviewed in detail. In this section, the data processing methods [192] and analyzing techniques [193], especially the AI-based methods (such as machine learning), are summarized according to different monitoring objectives. As shown in Fig. 11, the AI-based methods can be exploited to optimize the process parameters [194,195], predict the weld seam features [196,197], track the welding seam [198], adaptive control the welding process [199], classify weld defects [200] and validate the simulation results [156,201], etc. At the end of this section, in Table 3, the references are classified based on different monitoring objectives and AI techniques.

4.1. Process parameters optimization

Choosing appropriate process parameters is beneficial to obtain higher quality weld products. The Taguchi method and the AI-based techniques can effectively optimize the welding parameters [202], and the combination of these two methods can also obtain good optimized results [203,204]. Taguchi method is widely used in optimizing the process parameters, due to this approach can reduce the time and cost for the experimental investigations [205]. In [206], the optimal welding parameters were acquired by using the Taguchi method and applied the grey relational grade as the quality index. To improve the

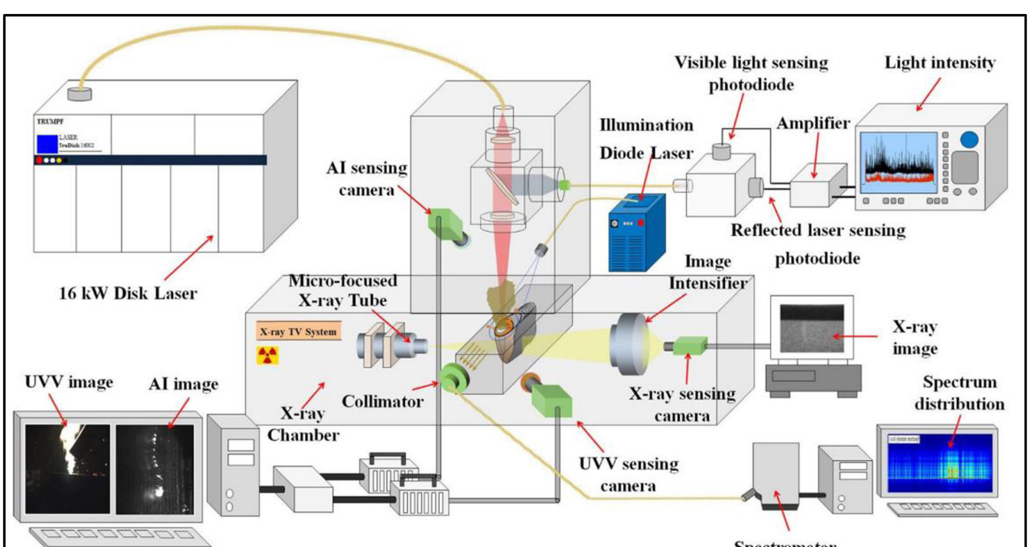

Fig. 10. The multiple sensing system which included six different sensors [189].

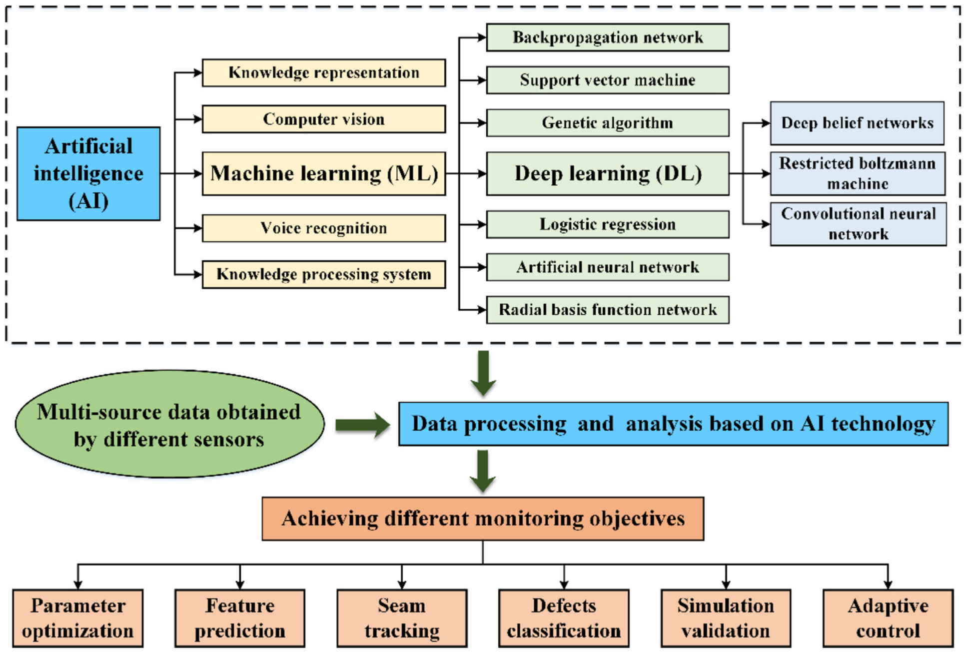

Fig. 11. A variety of AI-based technologies are used for data processing and analysis to achieve different monitoring objectives.

depth-width ratio of the weld seam, Ai et al. [207] applied the Taguchi method to optimize three welding parameters, i.e. the laser power, welding speed and focal position. Results showed the reliability and effectiveness of the proposed method. AI-based methods were also widely applied in parameter's optimization in recent years [208]. Cao et al. [209] used radial basis function neural network (RBFNN) and genetic algorithm (GA) to optimize the laser welding process parameters under the external magnetic field. The influences of different welding parameters, including the optimized parameters on the weld appearance, were analyzed, which showed that this method could effectively reduce the spatters. Rong et al. [210] combined the back-propagation neural network (BPNN) and GA to optimize the welding parameters. The Taguchi method was applied to design the welding experiments. Results indicated that this proposed method was helpful to improve the quality of the weld joint. Yang et al. [211] exploited the metamodels and non-dominated sorting genetic algorithm to acquire optimum process parameters of laser welding. The core optimization principle was to make full use of the prediction ability of the metamodels (i.e., Kriging, RBF, and support vector regression (SVR)). By using the AI-based or hybrid methods to optimize the process parameters, the quality of the weld seam can be improved effectively [212].

4.2. Seam features prediction

The appearance of the weld seam is the external manifestation of the welding quality. The weld seam features, such as the width of the weld seam and the penetration depth, etc, which can be predicted accurately by establishing the relationship with the monitoring signals [134,213]. Lee et al. [214] observed the acoustic signal in real-time, and the BPNN was used to predict the weld seam features. Results showed that the outputs of the prediction model agree well with the measured data of actual welding experiment. The principal component analysis (PCA) algorithm is commonly used in data processing, due to the outstanding ability in identifying the spectral line, extracting the spectral features and removing the data redundancy [215]. Gao et al. [216] used the PCA to reduce the data redundancy by analyzing the characteristics of the shadows of the molten pool which were defined and obtained in [141]. Then, the GA improved BPNN method was established to model the relation between the appearance of the weld seam and the obtained characteristics. Zhang et al. [217] monitored the electrode displacement signal and applied the image processing method to convert the obtained signals into binary images. By adopting the probabilistic neural network (PNN), the weld quality can be analyzed in a probabilistic viewpoint, and obtained deterministic classification results. To estimate the dynamic shape of the keyhole and the weld defects in on-line process, Luo et al. [218] applied a coaxial monitoring system to observe the keyhole shape in real time when the welding parameters changed suddenly, which provided the input data to the state observer based on RBFNN, and the potential welding porosities could be also indicated. Gao et al. [196] compared the prediction performance with BPNN and RBFNN at different welding speed in laser welding process. In [219], the effects of the multiple linear regression analysis and BPNN were contrasted by Wang et al.. The results in above two references showed that the BPNN model works better. Gunther et al. [220] applied reinforcement learning and deep learning techniques to monitoring systems. This monitoring system has a certain learning ability and can be adapted to different welding environments. Laying the foundation for the development of more intelligent monitoring systems.

4.3. Weld seam tracking

Laser welding process needs high precision of the laser beam positioning on the workpiece to ensure the high accuracy of welding trajectory and feed rate [221]. The seam-tracking devices and techniques [222,223], such as the IR imaging technology [224], the vision tracking technique [225] (i.e. machine vision [226]) and the artificial vision technology [227] are researched a lot to fulfill this requirement. During the multi-pass welding with traditional teaching and playback robot, it is difficult to obtain a stable weld seam. Gu et al. [228] devised an automatic welding tracking system to conquer the inadequacies of the traditional welding robot. The fuzzy-P controller was applied to control the welding torch to adjust its position in real-time to achieve accurate tracking of the weld seam. Vision capability of the monitoring system can supply reliable real-time seam tracking information. Nele et al. [229] used a CCD camera-based seam tracking system to acquire continuous images to extract and analyze the location and characteristics of the weld seam in real-time. The recognition accuracy of this automatic tracking system was verified and improved by the welding experiments. Results showed that this method could realize the seam gap detecting

Table 3
Paper's classification based on different monitoring objective and AI technique.

	Parameter optimization	Feature prediction	Seam tracking	Defects classification	Simulation validation	Adaptive control
AI technique	RBFNN, SVR, BPNN, ANN, DL, GA	RBFNN, SVR, BPNN, FNN, GA, PCA, DL, ANFIS	KF, RBFNN	RBFNN, SVM, SVM-CV, DL	Only monitoring	DL, Cellular Neural Networks (CNN), ANFIS, Adaptive bilinear model predictive control algorithm
reference	14, 32 − 33, 35, 48, 189 − 190, 197 − 207	33, 36, 43 − 44, 46, 67 − 68, 94, 108, 167, 175, 179, 188, 191 − 192, 208 − 215	6, 34, 38, 64, 105, 161, 163 − 164, 193, 216 − 224	16, 37, 116, 195, 228 − 241	53, 151, 196, 242 − 254	39, 42, 59, 61, 85, 194, 256 − 269
Useful AI technique	GA	BPNN, DL	KF	SVM, DL	/	DL, ANFIS

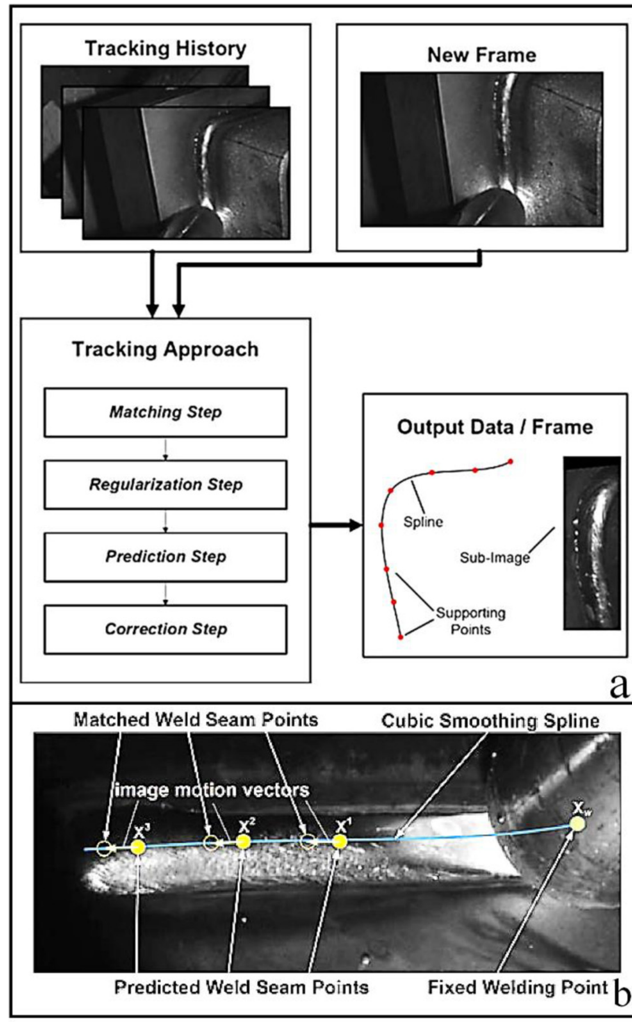

Fig. 12. (a) The weld seam tracking approach. (b) Weld seam point prediction. [233].

and weld seam tracking with high accuracy. Shi et al. [230] applied an efficient algorithm to achieve the weld seam detection from a single image during the butt joint welding. The basic idea of this approach was using the iterative edge detection and edge linking method to search the remnant edge to get the entire weld seam. Gao et al. [231] improved the adaptive Kalman filter (KF) system with the Elman neural network and utilized an error estimator to compensate for the filter error. Then in [232], the KF was improved by RBFNN. The actual welding experiments demonstrated that the KF compensated by the RBFNN could effectively track the weld seam and reduce the disturbance influences caused by the colored noises. Gao et al. also researched seam tracking method based on MOI technology [66,198]. Heber et al. [233] analyzed the high-quality image to extract the dynamic information during an ongoing welding process to track the position of the weld seam automatically. Fig. 12 introduced the principle of real-time seam tracking based on this method in detail. As can be seen from the figure, the entire tracking approach is divided into four steps. Firstly, matching image areas of welds using robust template tracking method. Secondly, the spline-based regularization method was used to process the matching graph. Thirdly, predicting the new weld seam points along the spline. Finally, correcting the predicted points with adaptive weld model.

4.4. Defects classification

The outside or inside welding defects affect the quality of the weld products. By classifying and monitoring the defects during the welding process, the generation of weld defects can be reduced [234]. Vision-based detection system [235] combined with classification models such as support vector machine (SVM) [236] or NDI detection system such as ultrasonics [237] are commonly used to detect the weld defects like hamping [238], crack [239], spatters [240], underfill [241], undercut and blowout [37], etc. One merit of laser welding is the high-speed of welding. However, the weld periodical appearance defect, namely humping, are frequently generated during the high-speed welding process. You et al. [242] applied the photodiode and visual sensor to monitor the welding zone simultaneously, and the SVM was used to identify the weld defects. Results showed that this approach could efficiently inspect weld defects. Passini et al. [78] utilized the ultrasonic phased array system to detect the welding defects in thin aluminum weldments. This detection method can effectively identify the presence of grouped porosity by testing and verifying with the X-ray radiography system and the metallographic inspection method. Rodil et al. [243] monitored and analyzed the radiation of the electron-free plasma to detect the weld defects. Sumesh et al. [244] researched the correlation between the arc sound signal and the defects, i.e. lack of fusion and burn through. The data mining software was used to extract the statistical features of raw data. The J48 and random forest algorithms were applied to classify the welding products into three categories: the good welding, welding with lack of fusion, and welding with burn through. Zhang et al. [245] established the relationship between the spectroscopy signals and the welding defects. The wavelet packet transform method was used to reduce the pulse interference in monitoring curves. The proposed technique has been proved that it was feasible to detect welding perturbation and defects. Then in [246], their team researched the SVM-CV (cross-validation) classification method which could successfully identify the porosity defect from normal welding products with high accuracy. Gao et al. [247] combined the MOI method with the PCA and SVM algorithms to build the identification model to detect the weld cracks. This combination method can effectively extract the weld crack characteristics and improve the detection accuracy. Fig. 13 shows the actual samples of defects and their corresponding magneto-optical images.

4.5. Simulation validation

The laser welding numerical simulation model [248,249] helps to reveal the complex phenomena of the welding zone to understand better and control the welding process [250,251]. Fig. 14 demonstrated the effectiveness of the simulation model by directly comparing the simulation results with experimental images. The numerical technique is also a useful tool to identify the key process parameters and reduce possible weld defects [252]. Monitoring the welding process can provide massive, reliable data to improve the model accuracy and verify the model reliability [178,253]. In [254], the simulation results showed that there are periodic keyhole oscillations and complex fluid dynamics in the molten pool. The evaporation rates obtained in the simulations and experiments showed a good correlation. Abederrazak et al. [255] utilized the experiments and the finite volume method (FVM) to research the thermal phenomena during the dynamic formation of the molten pool. Zhao et al. [256] established a model of welding temperature field based on FEM to explore the relationship among the process parameters, the interface temperature, and the microstructure of the weld seam. The simulation results and experimental data showed that the temperature history of the measured points had a similar trend, which proved the validity of the model. And in [257], Kazemi et al. applied an improved heat source model to predict the cross-section data of the weld seam, and the prediction results were almost identical to the experimental results. During the laser welding process, the periodic vibration of the keyhole causes the weld seam to produce porosity defects which are difficult to observe directly. Pang et al. [258] proposed a quantitative model of porosity defects induced by the instability of keyhole to research the weld pool dynamics and the pore formation process. Comparing the experimental results, the simulated fluctuations of the keyhole depth could reflect the changing trend of the number of pores and the average pore size. In [259], the dynamic behaviors and the complicated mechanisms of metallic vapor plume were systematically studied based on the multiple timescales multiphase model. The dynamic changes of the temperature, pressure, and velocity, etc. of vapor plume under different process parameters were predicted theoretically. Zhang [260] established a three-dimensional numerical model coupled with a ray-tracing algorithm to explore the transient dynamics behavior of the keyhole, molten pool, and plume. The simulation results of the cross-section shape of the weld seam were in good agreement with the experimental results. Wu et al. [261] utilized the experimental results to improve the analytic model of the molten pool surface. The three-dimensional topography data of the molten pool surface was measured in the experiment to calibrate the size and shape of the molten pool calculated by the simulation model. The calibrated analytic model will provide the weld pool boundary and penetration data to control the welding parameters.

4.6. Process control

According to the on-line monitoring information of the welding process, the real-time adjustment measure can be carried out to ensure the stability of the welding process, that is to ensure the welding quality of the welding products [263–265]. There is a short delay from the

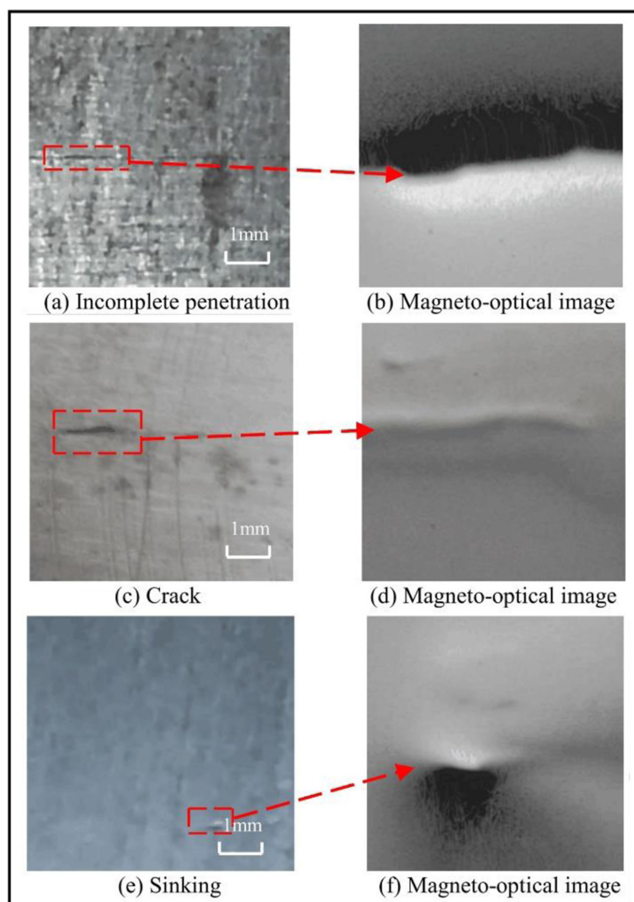

Fig. 13. Weld defects such as incomplete penetration, crack, and sinking were detected by MOI. [247].

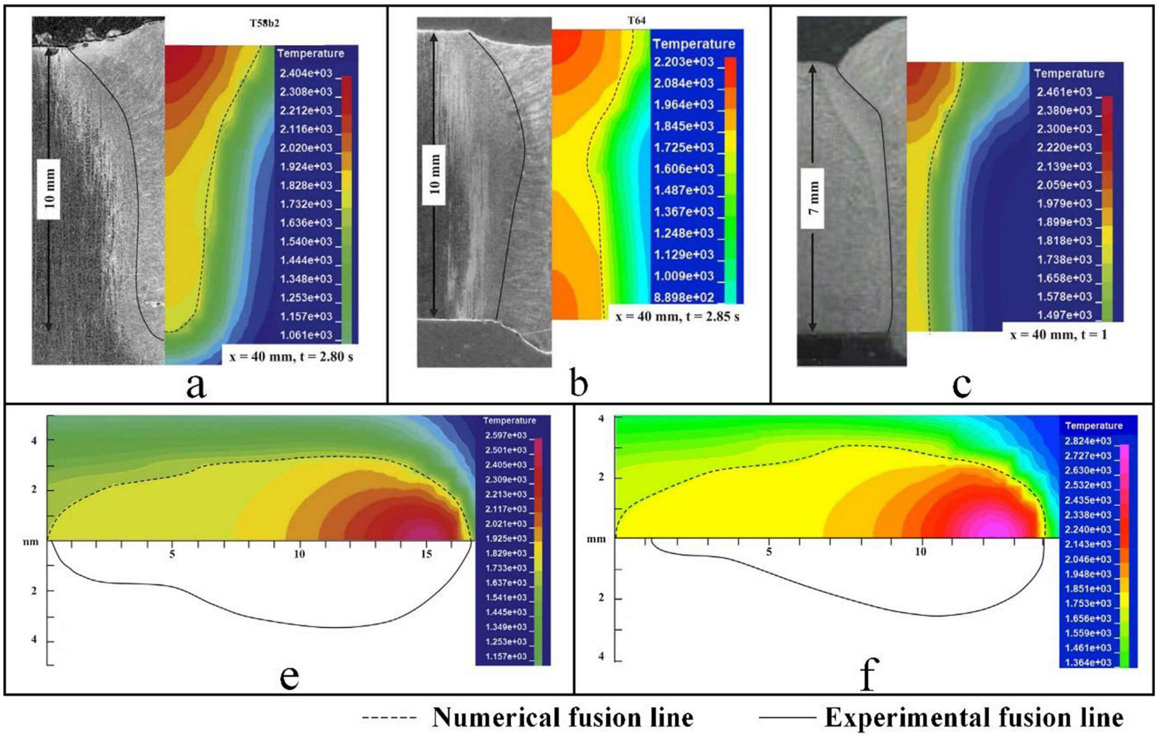

Fig. 14. The comparison results of the welding experiment and numerical simulation [262]: (a) and (e) case I: partial penetration, (b) and (f) case II: full penetration, (c) case III: full penetration.

acquisition of monitoring signal to the sending of adjusting signal, mainly the signal processing and analysis will take some time, so that the adjustment has a lag. However, with the progress of technology, less and less time is spent on data processing, which makes the real-time feedback control of welding process possible [28,266–268]. This monitoring-adjusting method makes the welding process more stable, improves the welding efficiency and product quality [269]. Hofman et al. [270] developed a control system based on the CMOS camera and software algorithms to adjust the laser power to maintain the stability of the molten pool width during welding process which can compensate the disturbances within a second. Craeghs et al. [271] devised a real-time monitoring and control system to observe the molten pool radiation continuously. The real-time control loop could provide effective feedback control of the welding process parameters by analyzing the signals from the photodiode and CMOS camera. Based on the experimental and theoretical research, Mrna et al. [272] proposed and implemented a feedback control method to adjust the laser welding process which can quickly optimize and control the focus of the laser beam. In [273], an efficient closed-loop control system was established, which can adjust the laser power in real-time to maintain the required penetration depth by monitoring the plasma electron temperature under different experimental conditions. Li et al. [274] established a weld penetration monitoring system based on the proportional integral derivative (PID) algorithm for penetration feedback provided by the penetration model, which related the weld penetration to the parent metal current. Experimental results verified the effectiveness of this method. Skilled welders can estimate and control the shape of the weld seam to obtain good welding products based on the observation of the molten pool. Liu et al. [275–277] conducted in-depth research on the welding process of welders to establish a smarter and more advanced control system to control the penetration of the weld seam. The skilled welder's welding process was simulated by the adaptive neuro-fuzzy inference system (ANFIS). The three-dimensional vision sensing system was used as the eye of the intelligent welding system to measure the characteristic parameters of the molten pool in real-time. The welding experiments proved that the developed control system could effectively achieve the ideal weld penetration under various disturbances and initial conditions.

5. Potential research issues and challenges

Intelligent laser welding technology can further improve welding efficiency and welding quality, which is an important part of intelligent manufacturing. In the big data manufacturing environment of intelligent manufacturing, the intelligent monitoring system [278] is just like the quality inspection workers, monitoring and adjusting the welding status in real time. The future potential research points of intelligent monitoring should focus on three aspects: intelligent acquisition platform of multiple welding signals, in-depth analysis and fusion of signals, and feedback control of welding parameters. That is to say, the whole process of welding monitoring (obtaining signal, analyzing signal and realizing monitoring target) will be more humanized.

5.1. Multiple welding signals collecting platform

A multi-sensor platform is like a worker's sensory system, which can collect multiple signals at the same time. However, the increase in the number of sensors will lead to problems such as difficulty in controlling multiple sensors simultaneously. Moreover, the sensors may be affected by many uncertainties. The multi-signal collecting system should be more intelligent, which can efficiently coordinate multiple sensors and be able to have a certain ability to reduce environmental interference.

5.2. Multi-source welding data deep analysis and fusion

Data fusion technology has been widely used in multi-sensor environments and can process and analyze data from different sensors simultaneously. Just like the human brain, multi-source data from sensing systems can be analyzed quickly and accurately. There are lots of issues that make deep data fusion a challenging task. The majority of these issues arise from the data to be fused, imperfection, and diversity of the sensor technologies, and the nature of the application environment. Many kinds of signals, such as optical, electric, acoustic, and thermal, are produced during the welding process. It is difficult to fusion these different types of data. Moreover, signal acquisition with different types of sensors also increases the difficulty of signal fusion, due to the obtained multi-signal have different characteristics. Furthermore, it is promising to combine the simulation data with actual sensor information by multi-fidelity surrogate model [284] and deep data mining [283] to obtain deeper information.

5.3. Welding parameters feedback control

The dynamic adjustment of welding parameters can effectively deal with the uncertain factors in the welding process, which is conducive to the stability of welding quality. Real time control of welding parameters is also helpful to reduce the occurrence of welding defects [279]. The interest in feedback control systems and adaptive processes has increased in recent years. The fused real-time monitoring signals are applied for feedback controlling the process parameters (e.g., laser power, welding speed, focus, feed rate). Feedback control methods are essential for ensuring the quality of the weld seam as they can react to dynamic fluctuations during the welding process. However, with the continuous improvement of welding equipment, the process parameters such as the welding power will be higher, and the welding speed will be faster, which requires a more responsive and adaptable control system. Humanized and intelligent process control technology is the key to further improve the welding quality [280].

6. Conclusion

In this paper, the development and investigation of sensors, new equipment and AI-based methods for real-time monitoring of welding quality are reviewed in detail. Firstly, the welding monitoring process is introduced. In-process monitoring technology is the most ideal real-time monitoring method. Because the monitoring information obtained in the in-process stage can be used to adjust the welding quality in real-time. Then, different kinds of monitoring equipment are classified and reviewed. Visual sensors are widely used because they can provide a more complete view of spatial information. ICI monitoring method can obtain real-time keyhole depth data, which is very important monitoring information for judging weld penetration. In order to make up for the deficiency of single sensor in performance, the multi-sensor monitoring technology is becoming more and more mature, which is the most commonly used monitoring method for researchers. Finally, the AI-based methods applied in welding monitoring is summarized. AI technology is the current research highlight, especially deep learning. It has great potential in data processing and mining, and can help to achieve various monitoring objectives. Therefore, developing an intelligent quality assessment system is the most interesting and challenging field.

Declaration of Competing Interest

The authors declare that they have no known competing financial interests or personal relationships that could have appeared to influence the work reported in this paper.

Acknowledgments

This research has been supported by the National Natural Science Foundation of China (NSFC) under Grant No. 51861165202 and No. 51721092, and the Fundamental Research Funds for the Central Universities, HUST: 2019JYCXJJ024.

References

[1] Stavridis J, Papacharalampopoulos A, Stavropoulos P. Quality assessment in laser welding: a critical review. Int J Adv Manuf Technol 2017;94:1825–47. https://doi.org/10.1007/s00170-017-0461-4.
[2] Bagger C, Olsen FO. Review of laser hybrid welding. J Laser Appl 2005;17:2–14. https://doi.org/10.2351/1.1848532.
[3] Sparkes M, Steen WM. "Light" industry: an overview of the impact of lasers on manufacturing. 2018. p. 1–22.
[4] Chen GY, Mei LF, Zhang MJ, Zhang Y, Wang ZJ. Research on key influence factors of laser overlap welding of automobile body galvanized steel. Opt Laser Technol 2013;45:726–33. https://doi.org/10.1016/j.optlastec.2012.05.002.
[5] Hong KM, Shin YC. Prospects of laser welding technology in the automotive industry: a review. J Mater Process Technol 2017;245:46–69. https://doi.org/10.1016/j.jmatprotec.2017.02.008.
[6] Pritschow PG, Haug K. Robust laser-stripe sensor for automated weld-seam-tracking in the shipbuilding industry. Proceedings of the 24th Annual Conference of the IEEE 1998;2:1236–41.
[7] Abderrazak K, Ben Salem W, Mhiri H, Bournot P, Autric M. Nd:YAG laser welding of AZ91 magnesium alloy for aerospace industries. Metall Mater Trans B 2009;40:54–61. https://doi.org/10.1007/s11663-008-9218-7.
[8] Pariona MM, Teleginski V, Santos Kd, Machado S, Zara AJ, Zurba NK, et al. Yb-fiber laser beam effects on the surface modification of Al–Fe aerospace alloy obtaining weld filet structures, low fine porosity and corrosion resistance. Surf Coat Technol 2012;206:2293–301. https://doi.org/10.1016/j.surfcoat.2011.10.007.
[9] Harman G, Albers J. The ultrasonic welding mechanism as applied to aluminum- and gold-wire bonding in microelectronics. Ieee Trans Parts Hybrids Packag 1977;13:406–12. https://doi.org/10.1109/tphp.1977.1135225.
[10] Arnold G. Laser Micro Manufacturing: Fast and Reliable Solutions for Joining, Drilling and Structuring. Laser Tech J 2009;6:16–9. https://doi.org/10.1002/latj.200990001.
[11] Tapia G, Elwany A. A review on process monitoring and control in metal-based additive manufacturing. J Manuf Sci Eng 2014;136:60–801. https://doi.org/10.1115/1.4028540.
[12] Amanat N, James NL, McKenzie DR. Welding methods for joining thermoplastic polymers for the hermetic enclosure of medical devices. Med Eng Phys 2010;32:690–9. https://doi.org/10.1016/j.medengphy.2010.04.011.
[13] Li K, Lu FG, Cui HC, Li XB, Tang XH, Li ZG. Investigation on the effects of shielding gas on porosity in fiber laser welding of T-joint steels. Int J Adv Manuf Technol 2015;77:1881–8. https://doi.org/10.1007/s00170-014-6538-4.
[14] Altarazi S, Hijazi L, Kaiser E. Process parameters optimization for multiple-inputs-multiple-outputs pulsed Green laser welding via response surface methodology. 2016 IEEE International Conference on industrial engineering and engineering management (IEEM) 2016:1041–5.
[15] You DY, Gao XD, Katayama S. Review of laser welding monitoring. Sci Technol Weld Join 2013;19:181–201. https://doi.org/10.1179/1362171813Y.0000000180.
[16] Zhang ZF, Chen SB. Real-time seam penetration identification in arc welding based on fusion of sound, voltage and spectrum signals. J Intell Manuf 2014;28:207–18. https://doi.org/10.1007/s10845-014-0971-y.
[17] Zhao HB, Qi H. Vision-based keyhole detection in laser full penetration welding process. J Laser Appl 2016;28:022412https://doi.org/10.2351/1.4944003.
[18] Luo M, Shin YC. Vision-based weld pool boundary extraction and width measurement during keyhole fiber laser welding. Opt Lasers Eng 2015;64:59–70. https://doi.org/10.1016/j.optlaseng.2014.07.004.
[19] Sibillano T, Ancona A, Rizzi D, Lupo V, Tricarico L, Lugara PM. Plasma plume oscillations monitoring during laser welding of stainless steel by discrete wavelet transform application. Sensors (Basel) 2010;10:3549–61. https://doi.org/10.3390/s100403549.
[20] Kaplan AFH, Powell J. Spatter in laser welding. J Laser Appl 2011;23:032005https://doi.org/10.2351/1.3597830.
[21] Zhang L, Basantes-Defaz AC, Ozevin D, Indacochea E. Real-time monitoring of welding process using air-coupled ultrasonics and acoustic emission. Int J Adv Manuf Technol 2018;101:1623–34. https://doi.org/10.1007/s00170-018-3042-2.
[22] Lv N, Zhong JY, Chen HB, Lin T, Chen SB. Real-time control of welding penetration during robotic GTAW dynamical process by audio sensing of arc length. Int J Adv Manuf Technol 2014;74:235–49. https://doi.org/10.1007/s00170-014-5875-7.
[23] Xu PQ, Tang XH, Yao S. Application of circular laser vision sensor (CLVS) on welded seam tracking. J Mater Process Technol 2008;205:404–10. https://doi.org/10.1016/j.jmatprotec.2007.11.268.
[24] Wang T, Gao XD, Katayama S, Jin XL. Study of dynamic features of surface plasma in high-power disk laser welding. Plasma Sci Technol 2012;14:245–51. https://doi.org/10.1088/1009-0630/14/3/11.
[25] Sebestova H, Chmelickova H, Nozka L, Moudry J. Non-destructive real time monitoring of the laser welding process. J Mater Eng Perform 2012;21:764–9. https://doi.org/10.1007/s11665-012-0193-4.
[26] Brock C, Hohenstein R, Schmidt M. Optical 3D position sensor for the fast tracking of light sources. Phys Procedia 2010;5:437–45. https://doi.org/10.1016/j.phpro.2010.08.071.
[27] Speka M, Mattei S, Pilloz M, Ilie M. The infrared thermography control of the laser welding of amorphous polymers. Ndt E Int 2008;41:178–83. https://doi.org/10.1136/bmj.320.7247.1426.
[28] KaierLe S. Understanding the Laser process new approaches for process monitoring in laser materials Processing. 2010. p. 49–52.
[29] Chivel Y, Smurov I. On-line temperature monitoring in selective laser sintering/

melting. Phys Procedia 2010;5:515–21. https://doi.org/10.1016/j.phpro.2010.08.079.

[30] Kageler C, Schmidt M. Frequency-based analysis of weld pool dynamics and keyhole oscillations at laser beam welding of galvanized steel sheets. Phys Procedia 2010;5:447–53. https://doi.org/10.1016/j.phpro.2010.08.072.

[31] You DY, Gao XD, Katayama S. Multiple-optics sensing of high-brightness disk laser welding process. Ndt E Int 2013;60:32–9. https://doi.org/10.1016/j.ndteint.2013.07.005.

[32] Zhou Q, Jiang P, Shao XY, Gao ZM, Cao LC, Yue C, et al. Optimization of process parameters of hybrid laser–Arc welding onto 316L using ensemble of metamodels. Metall Mater Trans B 2016;47:2182–96. https://doi.org/10.1007/s11663-016-0664-3.

[33] Nagesh DS, Datta GL. Genetic algorithm for optimization of welding variables for height to width ratio and application of ANN for prediction of bead geometry for TIG welding process. Appl Soft Comput 2010;10:897–907. https://doi.org/10.1016/j.asoc.2009.10.007.

[34] Gao XD, Zhen RH, Xiao ZL, Katayama S. Modeling for detecting micro-gap weld based on magneto-optical imaging. J Manuf Syst 2015;37:193–200. https://doi.org/10.1016/j.jmsy.2015.07.001.

[35] Jiang P, Cao LC, Zhou Q, Gao ZM, Rong Y, Shao XY. Optimization of welding process parameters by combining Kriging surrogate with particle swarm optimization algorithm. Int J Adv Manuf Technol 2016;86:2473–83. https://doi.org/10.1007/s00170-016-8382-1.

[36] Subashini L, Vasudevan M. Adaptive neuro-fuzzy inference system (ANFIS)-Based models for predicting the weld bead width and depth of penetration from the infrared thermal image of the weld pool. Metall Mater Trans B 2011;43:145–54. https://doi.org/10.1007/s11663-011-9570-x.

[37] You DY, Gao XD, Katayama S. WPD-PCA-Based laser welding process monitoring and defects diagnosis by using FNN and SVM. Ieee Trans Ind Electron 2015;62:628–36. https://doi.org/10.1109/TIE.2014.2319216.

[38] Gao XD, Liu YH, You DY. Detection of micro-weld joint by magneto-optical imaging. Opt Laser Technol 2014;62:141–51. https://doi.org/10.1016/j.optlastec.2013.12.027.

[39] Blug A, Carl D, Höfler H, Abt F, Heider A, Weber R, et al. Closed-loop control of laser power using the full penetration hole image feature in aluminum welding processes. Phys Procedia 2011;12:720–9. https://doi.org/10.1016/j.phpro.2011.03.090.

[40] Dorsch F, Dorsch F, Braun H, Kessler S, Pfitzner D, Rominger V. Online characterization of laser beam welds by NIR-camera observation. Proceedings of SPIE 2013;8603:86030Rhttps://doi.org/10.1117/12.2004196.

[41] Kogel-Hollacher M, Schoenleber M, Bautze T, Moser R, Strebel M. Inline monitoring of laser processing: new industrial results with the low coherence interferometry sensor approach. Proceedings of SPIE 2016;9741:97410Rhttps://doi.org/10.1117/12.2208004.

[42] Liu YK, Zhang YM. Supervised learning of human welder behaviors for intelligent robotic welding. Ieee Trans Autom Sci Eng 2017;14:1532–41. https://doi.org/10.1109/TASE.2015.2453351.

[43] Acherjee B, Mondal S, Tudu B, Misra D. Application of artificial neural network for predicting weld quality in laser transmission welding of thermoplastics. Appl Soft Comput 2011;11:2548–55. https://doi.org/10.1016/j.asoc.2010.10.005.

[44] Knaak K. Machine learning as a comparative tool to determine the relevance of signal features in laser welding. 10TH CIRP Concerence on Photonic Technologies [LANE 2018] 74. Procedia CIRP; 2018. p. 623–7.

[45] Wasmer K, Le-Quang T, Meylan B, Vakili-Farahani F, Olbinado MP, Rack A, et al. Laser processing quality monitoring by combining acoustic emission and machine learning: a high-speed X-ray imaging approach. Procedia Cirp 2018;74:654–8. https://doi.org/10.1016/j.procir.2018.08.054.

[46] Zhang ZH, Li B, Zhang WF, Lu RD, Wada S, Zhang Y. Real-time penetration state monitoring using convolutional neural network for laser welding of tailor rolled blanks. J Manuf Syst 2020;54:348–60. https://doi.org/10.1016/j.jmsy.2020.01.006.

[47] Zhang YX, You DY, Gao XD, Zhang N, Gao PP. Welding defects detection based on deep learning with multiple optical sensors during disk laser welding of thick plates. J Manuf Syst 2019;51:87–94. https://doi.org/10.1016/j.jmsy.2019.02.004.

[48] Yang L, Ume IC. Measurement of weld penetration depths in thin structures using transmission coefficients of laser-generated Lamb waves and neural network. Ultrasonics 2017;78:96–109. https://doi.org/10.1016/j.ultras.2017.02.019.

[49] Gao XD, Sun Y, You DY, Xiao ZL, Chen XH. Multi-sensor information fusion for monitoring disk laser welding. Int J Adv Manuf Technol 2015;85:1167–75. https://doi.org/10.1007/s00170-015-8032-z.

[50] Lin CS, Huang YC, Chen SH, Hsu YL, Lin YC. The application of deep learning and image processing technology in laser positioning. Appl Sci 2018;8:1542. https://doi.org/10.3390/app8091542.

[51] Ribic B, Palmer TA, DebRoy T. Problems and issues in laser-arc hybrid welding. Int Mater Rev 2009;54:223–44. https://doi.org/10.1179/174328009X411163.

[52] Jr RWM. Principles of welding: processes, physics, chemistry, and metallurgy[M]. John Wiley & Sons; 1999.

[53] Katayama S, Kawahito Y, Mizutani M. Elucidation of laser welding phenomena and factors affecting weld penetration and welding defects. Phys Procedia 2010;5:9–17. https://doi.org/10.1016/j.phpro.2010.08.024.

[54] Janssen JN, Ewe A. The functioning of some transducers and sensors intended for robotized laser. 2011.

[55] Kawahito Y, Ohnishi T, Katayama S. In-process monitoring and feedback control for stable production of full-penetration weld in continuous wave fibre laser welding. J Phys D Appl Phys 2009;42:85501–8. https://doi.org/10.1088/0022-3727/42/8/085501.

[56] Katayama S. Defect formation mechanisms and preventive procedures in laser welding[M]. Handbook of laser welding technologies. 2013. p. 332–73.

[57] Luo Y, Zhu L, Han JT, Xie XJ, Wan R, Zhu Y. Study on the acoustic emission effect of plasma plume in pulsed laser welding. Mech Syst Signal Process 2019;124:715–23. https://doi.org/10.1016/j.ymssp.2019.01.045.

[58] Katayama S, Gapontsev DV, Kawahito Y, Kliner DA, Dawson JW, Tankala K. Elucidation of phenomena in high-power fiber laser welding and development of prevention procedures of welding defects. Proceedings of SPIE - The International Society for Optical Engineering (Proceedings of SPIE) 2009;7195:71951R.

[59] Kawahito Y, Mizutani M, Katayama S. High quality welding of stainless steel with 10 kW high power fibre laser. Sci Technol Weld Join 2013;14:288–94. https://doi.org/10.1179/136217108X372531.

[60] Meng W, Li Z, Lu F, Wu Y, Chen J, Katayama S. Porosity formation mechanism and its prevention in laser lap welding for T-joints. J Mater Process Technol 2014;214:1658–64. https://doi.org/10.1016/j.jmatprotec.2014.03.011.

[61] Zhang YM, Qian K. Bilinear model predictive control of plasma keyhole pipe welding process 136. J Manuf Sci E-T ASME; 2014:10.1115/1.4025337.

[62] Liu YK, Zhang YM. Control of 3D weld pool surface. Control Eng Pract 2013;21:1469–80. https://doi.org/10.1016/j.conengprac.2013.06.019.

[63] Maher MA, Webster PJL, Chiao JC, Leung BYC, Yu JXZ, Resnick PJ, et al. Coaxial real-time metrology and gas assisted laser micromachining: process development. stochastic behavior, and feedback control 2010;7590:759003https://doi.org/10.1117/12.842409.

[64] Blecher JJ, Galbraith CM, Van Vlack C, Palmer TA, Fraser JM, Webster PJL, et al. Real time monitoring of laser beam welding keyhole depth by laser interferometry. Sci Technol Weld Join 2014;19:560–4. https://doi.org/10.1179/1362171814Y.0000000225.

[65] Ji Y, Grindal AW, Webster PJL, Fraser JM. Real-time depth monitoring and control of laser machining through scanning beam delivery system. J Phys D Appl Phys 2015;48:155301https://doi.org/10.1088/0022-3727/48/15/155301.

[66] Gao XD, Chen YQ, You DY, Xiao ZL, Chen XH. Detection of micro gap weld joint by using magneto-optical imaging and Kalman filtering compensated with RBF neural network. Mech Syst Signal Process 2017;84:570–83. https://doi.org/10.1016/j.ymssp.2016.07.041.

[67] Gao XD, Na SJ. Detection of weld position and seam tracking based on Kalman filtering of weld pool images. J Manuf Syst 2005;24:1–12. https://doi.org/10.1016/S0278-6125(06)00002-1.

[68] dorSch F. Process sensor systems for laser beam welding. 2012.

[69] Yusof MFM, Ishak M, Ghazali MF. Feasibility of using acoustic method in monitoring the penetration status during the pulse Mode laser welding process. IOP Conference Series: Materials Science and Engineering 2017;238:012006.

[70] Lv N, Xu YL, Fang G, Yu XW. Research on welding penetration state recognition based on BP-Adaboost model for pulse GTAW welding dynamic process. Advanced Robotics & Its Social Impacts. 2016.

[71] Huang W, Kovacevic R. A neural network and multiple regression method for the characterization of the depth of weld penetration in laser welding based on acoustic signatures. J Intell Manuf 2009;22:131–43. https://doi.org/10.1007/s10845-009-0267-9.

[72] Huang W, Kovacevic R. Feasibility study of using acoustic signals for online monitoring of the depth of weld in the laser welding of high-strength steels. Proc Inst Mech Eng Part B J Eng Manuf 2009;223:343–61. https://doi.org/10.1243/09544054JEM1320.

[73] Luo Z, Liu W, Wang Z, Ao S. Monitoring of laser welding using source localization and tracking processing by microphone array. Int J Adv Manuf Technol 2015;86:21–8. https://doi.org/10.1007/s00170-015-8095-x.

[74] Ao1 SS, Luo Z, ZhAo CF, et al. Numerical and experimental study of the acoustic signal generated by vapour flow in laser welding 34. LASERS IN ENGINEERING; 2016. p. 145–65.

[75] Al-Sarraf Z, Lucas M. A study of weld quality in ultrasonic spot welding of similar and dissimilar metals. J Phys Conf Ser 2012;382:012013https://doi.org/10.1088/1742-6596/382/1/012013.

[76] Gu XP, Xu GC, Liu J, Gu XY, et al. Ultrasonic testing and evaluation of laser welds in stainless steel. Laser Eng 2013;26:103–13.

[77] Kustron P, Korzeniowski M, Lewandowski M, Witek B, Rozbicki J. A high frequency ultrasonic imaging of welded joints. IEEE International Ultrasonics Symposium. IEEE; 2016.

[78] Passini A, Oliveira ACd, Riva R, Travessa DN, Cardoso KR. Ultrasonic inspection of AA6013 laser welded joints. Mater Res 2011;14:417–22. https://doi.org/10.1590/S1516-14392011005000057.

[79] Mizota H, Nagashima Y, Obana T. Fundamental study of molten pool depth measurement method using an ultrasonic phased array system. Jpn J Appl Phys 2015;54:07HC03https://doi.org/10.7567/JJAP.54.07HC03.

[80] Sibillano T, Ancona A, Berardi V, Lugara PM. A real-time spectroscopic sensor for monitoring laser welding processes. Sensors (Basel) 2009;9:3376–85. https://doi.org/10.3390/s90503376.

[81] Sibillano T, Rizzi D, Ancona A, Saludes-Rodil S, Rodríguez Nieto J, Chmelíčková H, et al. Spectroscopic monitoring of penetration depth in CO2 Nd:YAG and fiber laser welding processes. J Mater Process Technol 2012;212:910–6. https://doi.org/10.1016/j.jmatprotec.2011.11.016.

[82] Ma H, Wei S, Lin T, Chen S, Li L. Binocular vision system for both weld pool and root gap in robot welding process. Sens Rev 2010;30:116–23. https://doi.org/10.1108/02602281011022706.

[83] Tenner F, Brock C, Hohenstein R, Zalevsky Z, Schmidt M. Remote optical detection of the fusion state in laser deep penetration welding. Phys Procedia 2013;41:515–9. https://doi.org/10.1016/j.phpro.2013.03.109.

[84] Gao XD, You DY, Katayama S. The high frequency characteristics of laser reflection

and visible light during solid state disk laser welding. Laser Phys Lett 2015;12. https://doi.org/10.1088/1612-2011/12/7/076003.
[85] Haran FM, Hand DP, Peters C, Jones J. Real-time focus control in laser welding. Meas Sci Technol 1996;7:1095–8. https://doi.org/10.1088/0957-0233/7/8/001.
[86] Eriksson I, Powell J, Kaplan AFH. Signal overlap in the monitoring of laser welding. Meas Sci Technol 2010;21:105705https://doi.org/10.1088/0957-0233/21/10/105705.
[87] Sibillano T, Ancona A, Rizzi D, Rodil SS, Nieto JR, Konuk AR, et al. Study on the correlation between plasma electron temperature and penetration depth in laser welding processes. Phys Procedia 2010;5:429–36. https://doi.org/10.1016/j.phpro.2010.08.070.
[88] Konuk AR, Aarts RGKM, in'tVeld AJH, Sibillano T, Rizzi D, Ancona A. Process control of stainless steel laser welding using an optical spectroscopic sensor. Phys Procedia 2011;12:744–51. https://doi.org/10.1016/j.phpro.2011.03.093.
[89] Rizzi D, Sibillano T, Pietro Calabrese P, Ancona A, Mario Lugarà P. Spectroscopic, energetic and metallographic investigations of the laser lap welding of AISI 304 using the response surface methodology. Opt Lasers Eng 2011;49:892–8. https://doi.org/10.1016/j.optlaseng.2011.02.014.
[90] Zaeh MF, Huber S. Characteristic line emissions of the metal vapour during laser beam welding. Prod Eng 2011;5:667–78. https://doi.org/10.1007/s11740-011-0337-7.
[91] Zah MF, Huber S, et al. In-situ melt identification during laser beam welding. International Congress on Applications of Lasers & Electro-Optics 2010;2010:1317–22.
[92] Zaeh MF, Reinhart G, Ostgathe M, et al. A holistic approach for the cognitive control of production systems. Adv Eng Inform 2010;24:300–7. https://doi.org/10.1016/j.aei.2010.05.014.
[93] Mrna L, Sarbort M, Rerucha S, Jedlicka P. Correlation between the keyhole depth and the frequency characteristics of light emissions in laser welding. Phys Procedia 2013;41:469–77. https://doi.org/10.1016/j.phpro.2013.03.103.
[94] De Bono P, Allen C, D'Angelo G, Cisi A. Investigation of optical sensor approaches for real-time monitoring during fibre laser welding. J Laser Appl 2017;29. https://doi.org/10.2351/1.4983253.
[95] Liu XF, Jia CB, Wu CS, Zhang GK, Gao JQ. Measurement of the keyhole entrance and topside weld pool geometries in keyhole plasma arc welding with dual CCD cameras. J Mater Process Technol 2017;248:39–48. https://doi.org/10.1016/j.jmatprotec.2017.05.012.
[96] Roozbahani H, Marttinen P, Salminen A. Real-time monitoring of laser scribing process of CIGS solar panels utilizing high speed camera. Ieee Photonics Technol Lett 2018:1. https://doi.org/10.1109/LPT.2018.2867274.
[97] Wang T, Chen JQ, Gao XD, Li W. Quality monitoring for laser welding based on high-speed photography and support vector machine. Appl Sci 2017;7:299. https://doi.org/10.3390/app7030299.
[98] Lee SK, Na SJ. A study on automatic seam tracking in pulsed laser edge welding by using a vision sensor without an auxiliary light source. J Manuf Syst 2002;21:302–15. https://doi.org/10.1016/S0278-6125(02)80169-8.
[99] Gao XD, Wen Q, Katayama S. Analysis of high-power disk laser welding stability based on classification of plume and spatter characteristics. Trans Nonferrous Met Soc China 2013;23:3748–57. https://doi.org/10.1016/S1003-6326(13)62925-8.
[100] Zhang Y, Zhang CL, Tan LP, Li SC. Coaxial monitoring of the fibre laser lap welding of Zn-coated steel sheets using an auxiliary illuminant. Opt Laser Technol 2013;50:167–75. https://doi.org/10.1016/j.optlastec.2013.03.001.
[101] Brock C, Tenner F, Klampfl F, Hohenstein R, Schmidt M. Detection of weld defects by high speed imaging of the vapor plume. Phys Procedia 2013;41:539–43. https://doi.org/10.1016/j.phpro.2013.03.113.
[102] Gao XD, Zhang YX. Monitoring of welding status by molten pool morphology during high-power disk laser welding. Opt – Int J Light Electron Opt 2015;126:1797–802. https://doi.org/10.1016/j.ijleo.2015.04.060.
[103] Zhang Y, Li FZ, Liang ZC, Ying YY, Lin QD, Wei HY. Correlation analysis of penetration based on keyhole and plasma plume in laser welding. J Mater Process Technol 2018;256:1–12. https://doi.org/10.1016/j.jmatprotec.2018.01.032.
[104] Kim CH, Ahn DC. Coaxial monitoring of keyhole during Yb:YAG laser welding. Opt Laser Technol 2012;44:1874–80. https://doi.org/10.1016/j.optlastec.2012.02.025.
[105] Tenner F, Berg B, Brock C, Klämpfl F, Schmidt M. Experimental approach for quantification of fluid dynamics in laser metal welding. J Laser Appl 2015;27. https://doi.org/10.2351/1.4906302.
[106] Liu ZM, Wu CS, Chen MA. Visualizing the influence of the process parameters on the keyhole dimensions in plasma arc welding. Meas Sci Technol 2012;23:105603https://doi.org/10.1088/0957-0233/23/10/105603.
[107] Ilar T, Eriksson I, Powell J, Kaplan A. Root humping in Laser Welding – an investigation based on high speed imaging. Phys Procedia 2012;39:27–32. https://doi.org/10.1016/j.phpro.2012.10.010.
[108] Kaierle S. Process monitoring and control of laser beam welding. Laser Technik Journal; 2008. p. 41–3.
[109] Ye Z, Fang G, Chen SB, Zou JJ. Passive vision based seam tracking system for pulse-MAG welding. Int J Adv Manuf Technol 2012;67:1987–96. https://doi.org/10.1007/s00170-012-4625-y.
[110] Kong F, Ma J, Carlson B, Kovacevic R. Real-time monitoring of laser welding of galvanized high strength steel in lap joint configuration. Opt Laser Technol 2012;44:2186–96. https://doi.org/10.1016/j.optlastec.2012.03.003.
[111] Zhang GK, Wu CS, Liu XF. Single vision system for simultaneous observation of keyhole and weld pool in plasma arc welding. J Mater Process Technol 2015;215:71–8. https://doi.org/10.1016/j.jmatprotec.2014.07.033.
[112] Chen JQ, Wang T, Gao XD, Wei L. Real-time monitoring of high-power disk laser welding based on support vector machine. Comput Ind 2018;94:75–81. https://doi.org/10.1016/j.compind.2017.10.003.
[113] Liu XF, Wu CS, Jia CB, Zhang GK. Visual sensing of the weld pool geometry from the topside view in keyhole plasma arc welding. J Manuf Process 2017;26:74–83. https://doi.org/10.1016/j.jmapro.2017.01.011.
[114] Wang L, Gao XD, Chen ZQ. Status analysis of keyhole bottom in laser-MAG hybrid welding process. Opt Express 2018;26:347–55. https://doi.org/10.1364/OE.26.000347.
[115] Zhang LJ, Zhang JX, Gumenyuk A, Rethmeier M, Na SJ. Numerical simulation of full penetration laser welding of thick steel plate with high power high brightness laser. J Mater Process Technol 2014;214:1710–20. https://doi.org/10.1016/j.jmatprotec.2014.03.016.
[116] You DY, Gao XD, Katayama S. Visual-based spatter detection during high-power disk laser welding. Opt Lasers Eng 2014;54:1–7. https://doi.org/10.1016/j.optlaseng.2013.09.010.
[117] Chen FX, Chen X, Xie X, Feng X, Yang LX. Full-field 3D measurement using multi-camera digital image correlation system. Opt Lasers Eng 2013;51:1044–52. https://doi.org/10.1016/j.optlaseng.2013.03.001.
[118] Fan CJ, Lv FL, Chen SB. Visual sensing and penetration control in aluminum alloy pulsed GTA welding. Int J Adv Manuf Technol 2008;42:126–37. https://doi.org/10.1007/s00170-008-1587-1.
[119] Liu ZM, Wu CS, Gao JQ. Vision-based observation of keyhole geometry in plasma arc welding. Int J Therm Sci 2013;63:38–45. https://doi.org/10.1016/j.ijthermalsci.2012.07.006.
[120] von Witzendorff P, Kaierle S, Suttmann O, Overmeyer L. Using pulse shaping to control temporal strain development and solidification cracking in pulsed laser welding of 6082 aluminum alloys. J Mater Process Technol 2015;225:162–9. https://doi.org/10.1016/j.jmatprotec.2015.06.007.
[121] Chen ZQ, Gao XD, Katayama S, Xiao Z, Chen X. Elucidation of high-power disk laser welding phenomena by simultaneously observing both top and bottom of weldment. Int J Adv Manuf Technol 2016;88:1141–50. https://doi.org/10.1007/s00170-016-8837-4.
[122] Dowden J, Kapadia P, Clucas A, Ducharme R, Steen WM. On the relation between fluid dynamic pressure and the formation of pores in laser keyhole welding. J Laser Appl 1996;8:183–90. https://doi.org/10.2351/1.4745420.
[123] Huang RS, Liu LM, Song G. Infrared temperature measurement and interference analysis of magnesium alloys in hybrid laser-TIG welding process. Mater Sci Eng A 2007;447:239–43. https://doi.org/10.1016/j.msea.2006.10.069.
[124] Uspenskiy SA, Shcheglov PY, Petrovskiy VN, Gumenyuk AV, Rethmeier M. Spectral diagnostics of a vapor-plasma plume produced during welding with a high-power ytterbium fiber laser. Opt Spectrosc 2013;115:140–6. https://doi.org/10.1134/S0030400X13070205.
[125] Planck M. Zur Theorie des Gesetzes der Energieverteilung im Normalspektrum. Deutsche Physikalische Gesellschaft Verhandlungen 1900;2:237–45.
[126] Golubev VS, Dubrov AV, Zavalov YN, Dubrov VD. Diagnostics of laser radiance penetration into material by multi-channel pyrometer, Advanced Optoelectronics and Lasers (CAOL). 2010 International Conference on. 2010:182–4.
[127] Bertrand SI, Grevey P. Application of near infrared pyrometry for continuous Nd:YAG laser welding of stainless steel. Appl Surf Sci 2000;168(1–4):182–5. https://doi.org/10.1016/S0169-4332(00)00586-9.
[128] Wippo V, Devrient M, Kern M, Jaeschke P, Frick T, Stute U, et al. Evaluation of a pyrometric-based temperature measuring process for the laser transmission welding. Phys Procedia 2012;39:128–36. https://doi.org/10.1016/j.phpro.2012.10.022.
[129] Yamazaki K, Yamamoto E, Suzuki K, Koshiishi F, Waki K, Tashiro S, et al. The measurement of metal droplet temperature in GMA welding by infrared two-colour pyrometry. Weld Int 2010;24:81–7. https://doi.org/10.1080/09507110902842950.
[130] Kohler H, Thomy C, Vollertsen F. Contact-less temperature measurement and control with applications to laser cladding. Weld World 2015;60:1–9. https://doi.org/10.1007/s40194-015-0275-7.
[131] Doubenskaia BP, Pinon M, et al. On-line optical monitoring of Nd:YAG laser lap welding of Zn-coated steel sheets. IV International WLT-Conference on Lasers in Manufacturing 2007:547–52.
[132] Gade R, Moeslund TB. Thermal cameras and applications: a survey. Mach Vis Appl 2013;25:245–62. https://doi.org/10.1007/s00138-013-0570-5.
[133] Chokkalingham S, Chandrasekhar N, Vasudevan M. Predicting the depth of penetration and weld bead width from the infra red thermal image of the weld pool using artificial neural network modeling. J Intell Manuf 2011;23:1995–2001. https://doi.org/10.1007/s10845-011-0526-4.
[134] Chandrasekhar N, Vasudevan M, Bhaduri AK, Jayakumar T. Intelligent modeling for estimating weld bead width and depth of penetration from infra-red thermal images of the weld pool. J Intell Manuf 2013;26:59–71. https://doi.org/10.1007/s10845-013-0762-x.
[135] Weberpals J, Hermann T, Berger P, Singpiel H. Utilisation of thermal radiation for process monitoring. Phys Procedia 2011;12:704–11. https://doi.org/10.1016/j.phpro.2011.03.088.
[136] Chen ZQ, Gao XD. Detection of weld pool width using infrared imaging during high-power fiber laser welding of type 304 austenitic stainless steel. Int J Adv Manuf Technol 2014;74:1247–54. https://doi.org/10.1007/s00170-014-6081-3.
[137] Lehmann PH, Chmelickova H, Osten W, Sebestova H, Havelkova M, Albertazzi A, et al. Laser Welding Control Monitoring Plasma 2013;8788:87882P. https://doi.org/10.1117/12.2021864.
[138] Chen GY, Zhang MJ, Zhao Z, Zhang Y, Li SC. Measurements of laser-induced plasma temperature field in deep penetration laser welding. Opt Laser Technol 2013;45:551–7. https://doi.org/10.1016/j.optlastec.2012.05.033.
[139] Beyer E, Dorsch F, Morris T, Braun H, Kessler S, Pfitzner D, et al. NIR-camera-

based online diagnostics of laser beam welding processes, high power laser materials processing: lasers, beam delivery, Diagnostics, and applications. Int Soc Opt. Phot 2012;8239:82390T. https://doi.org/10.1117/12.908646.
[140] Zhang WJ, Zhang X, Zhang YM. Robust pattern recognition for measurement of three dimensional weld pool surface in GTAW. J Intell Manuf 2013;26:659–76. https://doi.org/10.1007/s10845-013-0825-z.
[141] Zhang YX, Gao XD. Analysis of characteristics of molten pool using cast shadow during high-power disk laser welding. Int J Adv Manuf Technol 2013;70:1979–88. https://doi.org/10.1007/s00170-013-5442-7.
[142] Boley WR, Graf M. Online detection of Pore formation during laser DeepPenetration welding. Proceeding of Lasers in Manufacturing Congress (LIM) Google Scholar 2015.
[143] Bautze T, Markus KH. Keyhole Depth is just a Distance: the IDM sensor improves laser welding processes. Laser Tech J 2014;11:39–43. https://doi.org/10.1002/latj.201400040.
[144] Kim J, Ki H. Scaling law for penetration depth in laser welding. J Mater Process Technol 2014;214:2908–14. https://doi.org/10.1016/j.jmatprotec.2014.06.025.
[145] Zhao C, Fezzaa K, Cunningham RW, Wen H, De Carlo F, Chen LY, et al. Real-time monitoring of laser powder bed fusion process using high-speed X-ray imaging and diffraction. Sci Rep 2017;7:3602. https://doi.org/10.1038/s41598-017-03761-2.
[146] Webster PJL, Wright LG, Ji Y, Galbraith CM, Kinross AW, Van Vlack C, et al. Automatic laser welding and milling with in situ inline coherent imaging. Opt Lett 2014;39:6217–20. https://doi.org/10.1364/OL.39.006217.
[147] West M, Ellis AT, Potts PJ, Streli C, Vanhoof C, Wobrauschek P. Atomic Spectrometry Update – a review of advances in X-ray fluorescence spectrometry and their applications. J Anal At Spectrom 2015;30(2015):1839–89. https://doi.org/10.1039/c5ja90033f.
[148] Schluter S, Sheppard A, Brown K, Wildenschild D. Image processing of multiphase images obtained via X-ray microtomography: a review. Water Resour Res 2014;50:3615–39. https://doi.org/10.1002/2014WR015256.
[149] Xu W, Frantti T. Adaptive real-time fuzzy X-Ray solder joint inspection system. J Manuf Syst 2002;21:111–25. https://doi.org/10.1016/S0278-6125(02)80005-X.
[150] Hallouard F, Anton N, Choquet P, Constantinesco A, Vandamme T. Iodinated blood pool contrast media for preclinical X-ray imaging applications–a review. Biomaterials 2010;31:6249–68. https://doi.org/10.1016/j.biomaterials.2010.04.066.
[151] Doude H, Schneider J, Patton B, Stafford S, Waters T, Varner C. Optimizing weld quality of a friction stir welded aluminum alloy. J Mater Process Technol 2015;222:188–96. https://doi.org/10.1016/j.jmatprotec.2015.01.019.
[152] Taina IA, Heck RJ, Elliot TR. Application of X-ray computed tomography to soil science: a literature review. Can J Soil Sci 2008;88:1–19. https://doi.org/10.4141/CJSS06027.
[153] Vanska M, Abt F, Weber R, Salminen A, Graf T. Effects of welding parameters onto keyhole geometry for partial penetration laser welding. Phys Procedia 2013;41:199–208. https://doi.org/10.1016/j.phpro.2013.03.070.
[154] Abt F, Boley M, Weber R, Graf T, Popko G, Nau S. Novel X-ray system for in-situ diagnostics of laser based processes – first experimental results. Phys Procedia 2011;12:761–70. https://doi.org/10.1016/j.phpro.2011.03.095.
[155] Yan J, Gao M, Zeng XY. Study on microstructure and mechanical properties of 304 stainless steel joints by TIG, laser and laser-TIG hybrid welding. Opt Lasers Eng 2010;48:512–7. https://doi.org/10.1016/j.optlaseng.2009.08.009.
[156] Kong FR, Kovacevic R. 3D finite element modeling of the thermally induced residual stress in the hybrid laser/arc welding of lap joint. J Mater Process Technol 2010;210:941–50. https://doi.org/10.1016/j.jmatprotec.2010.02.006.
[157] Norris JT, Robino CV, Hirschfeld DA, Perricone MJ. Effects of laser parameters on porosity formation: investigating millimeter scale continuous wave Nd:YAG laser welds. Weld J 2011;90:198S–203S.
[158] Duprize ND, Denkl A. Advances of OCT Technology for Laser Beam Processing: precision and quality during laser welding. Laser Tech J 2017;14:34–8. https://doi.org/10.1002/latj.201700021.
[159] Ackermann P, Schmitt R. Tomographical process monitoring of laser transmission welding with OCT. Conference Proceedings 2017;10329:103290Hhttps://doi.org/10.1117/12.2269108.
[160] Fraser JM. Laser process monitoring and automatic control at kHz rates through inline coherent imaging. American Institute of Physics; 2012. p. 492–6.
[161] Smith LM, Dobson CC. Absolute displacement measurements using modulation of the spectrum of white light in a Michelson interferometer. Appl Opt 1989;28:3339–42. https://doi.org/10.1364/AO.28.003339.
[162] Yu JXZ, Webster PJL, Leung BYC, Fraser JM, et al. High-quality percussion drilling of silicon with a CW fiber laser. Conference Proceedings 2010;7584. https://doi.org/10.1117/12.842616. 75840W.
[163] Pastor M, Zhao H, DebRoy T. Continuous wave-Nd: yttrium–aluminum–garnet laser welding of AM60B magnesium alloy. J Laser Appl 2000;12:91–100. https://doi.org/10.2351/1.521922.
[164] Webster PJL, Wright LG, Mortimer KD, Leung BY, Yu K, Fraser JM. Automatic real-time guidance of laser machining with inline coherent imaging. J Laser Appl 2011;23:022001https://doi.org/10.2351/1.3567955.
[165] Leung BY, Webster PJL, Fraser JM, Yang VX. Real-time guidance of thermal and ultrashort pulsed laser ablation in hard tissue using inline coherent imaging. Lasers Surg Med 2012;44:249–56. https://doi.org/10.1002/lsm.21162.
[166] Gao XD, Chen YQ. Detection of micro gap weld using magneto-optical imaging during laser welding. Int J Adv Manuf Technol 2014;73:23–33. https://doi.org/10.1007/s00170-014-5811-x.
[167] Xia TK, Hui PM, Stroud D. Theory of Faraday rotation in granular magnetic materials. J Appl Phys 1990;67:2736–41. https://doi.org/10.1063/1.345438.
[168] Gao XD, Huang GX, You DY, Lan CZ, Zhang NF. Magneto-optical imaging deviation model of micro-gap weld joint. J Manuf Syst 2017;42:82–92. https://doi.org/10.1016/j.jmsy.2016.11.005.
[169] Gao XD, Lan CZ, You DY, Li GH, Zhang NF. Weldment nondestructive testing using magneto-optical imaging induced by alternating magnetic field. J Nondestruct Eval 2017;36. https://doi.org/10.1007/s10921-017-0434-4.
[170] Todorov E, Nagy B, Levesque S, Ames N, Na J. Inspection of laser welds with array eddy current technique. AIP Conference Proceedings. 2013. p. 1065–72.
[171] Brock C, Hohenstein R, Schmidt M. Mechanisms of vapour plume formation in laser deep penetration welding. Opt Lasers Eng 2014;58:93–101. https://doi.org/10.1016/j.optlaseng.2014.02.001.
[172] Liu GQ, Gao XD, You DY, Zhang NF. Prediction of high power laser welding status based on PCA and SVM classification of multiple sensors. J Intell Manuf 2016;30:821–32. https://doi.org/10.1007/s10845-016-1286-y.
[173] Turichin G, Zemlyakov E, Babkin K, Kuznetsov A. Monitoring of laser and hybrid welding of steels and Al-alloys. Phys Procedia 2014;56:1232–41. https://doi.org/10.1016/j.phpro.2014.08.039.
[174] Li SC, Chen GY, Zhou C. Effects of welding parameters on weld geometry during high-power laser welding of thick plate. Int J Adv Manuf Technol 2015;79:177–82. https://doi.org/10.1007/s00170-015-6813-z.
[175] Liu W, Liu S, Ma JJ, Kovacevic R. Real-time monitoring of the laser hot-wire welding process. Opt Laser Technol 2014;57:66–76. https://doi.org/10.1016/j.optlastec.2013.09.026.
[176] Norman P, Engstrom H, Kaplan AFH. Theoretical analysis of photodiode monitoring of laser welding defects by imaging combined with modelling. J Phys D Appl Phys 2008;41:195502https://doi.org/10.1088/0022-3727/41/19/195502.
[177] Wang J, Wang CM, Meng XX, Hu XY, Yu YC, Yu SF. Interaction between laser-induced plasma/vapor and arc plasma during fiber laser-MIG hybrid welding. J Mech Sci Technol 2011;25:1529–33. https://doi.org/10.1007/s12206-011-0410-3.
[178] Volpp J. Keyhole stability during laser welding—part II: process pores and spatters. Prod Eng 2016;11:9–18. https://doi.org/10.1007/s11740-016-0705-4.
[179] Li SC, Chen GY, Katayama S, Zhang Y. Relationship between spatter formation and dynamic molten pool during high-power deep-penetration laser welding. Appl Surf Sci 2014;303:481–8. https://doi.org/10.1016/j.apsusc.2014.03.030.
[180] Wu D, Chen HB, He YS, Song S, Lin T, Chen SB. A prediction model for keyhole geometry and acoustic signatures during variable polarity plasma arc welding based on extreme learning machine. Sens Rev 2016;36:257–66. https://doi.org/10.1108/sr-01-2016-0009.
[181] Zhang P, Kong L, Liu WZ, Chen JJ, Zhou KB, et al. Real-time monitoring of laser welding based on multiple sensors. 20th Chinese Control and Decision Conference 2008:1746–8.
[182] Pal K, Pal SK. Monitoring of weld penetration using arc acoustics. Mater Manuf Process 2011;26:684–93. https://doi.org/10.1080/10426910903496813.
[183] Chen B, Wang JF, Chen SB. Modeling of pulsed GTAW based on multi-sensor fusion. Sens Rev 2009;29:223–32. https://doi.org/10.1108/02602280910967639.
[184] Chen B, Wang JF, Chen SB. Prediction of pulsed GTAW penetration status based on BP neural network and D-S evidence theory information fusion. Int J Adv Manuf Technol 2009;48:83–94. https://doi.org/10.1007/s00170-009-2258-6.
[185] Chen B, Wang JF, Chen SB. A study on application of multi-sensor information fusion in pulsed GTAW. Ind Robot Int J 2010;37:168–76. https://doi.org/10.1108/01439911011018948.
[186] Boley M, Abt F, Weber R, Graf T. X-ray and optical videography for 3D measurement of capillary and melt pool geometry in laser welding. Phys Procedia 2013;41:488–95. https://doi.org/10.1016/j.phpro.2013.03.105.
[187] Harooni M, Carlson B, Kovacevic R. Detection of defects in laser welding of AZ31B magnesium alloy in zero-gap lap joint configuration by a real-time spectroscopic analysis. Opt Lasers Eng 2014;56:54–66. https://doi.org/10.1016/j.optlaseng.2013.11.015.
[188] You DY, Gao XD, Katayama S. A novel stability quantification for disk laser welding by using frequency correlation coefficient between multiple-optics signals. Ieee/asme Trans Mechatron 2015;20:327–37. https://doi.org/10.1109/TMECH.2014.2311097.
[189] You DY, Gao XD, Katayama S. Data-driven based analyzing and modeling of MIMO laser welding process by integration of six advanced sensors. Int J Adv Manuf Technol 2015;82:1127–39. https://doi.org/10.1007/s00170-015-7455-x.
[190] Lee HK, Park SH, Kang CY. Effect of plasma current on surface defects of plasma-MIG welding in cryogenic aluminum alloys. J Mater Process Technol 2015;223:203–15. https://doi.org/10.1016/j.jmatprotec.2015.04.008.
[191] Oezmert A, Drenker A, Nazery V. Detectability of penetration based on weld pool geometry and process emission Spectrum in laser welding of copper. Phys Procedia 2013;41:509–14. https://doi.org/10.1016/j.phpro.2013.03.108.
[192] Zhang ZF, Wang GR, Chen SB. Member, IEEE, Multisensory Data Fusion technique and its application to welding process monitoring. Phys Procedia 2016;39:784–91. https://doi.org/10.1109/ARSO.2016.7736298.
[193] Wang XW, Li RR. Intelligent modelling of back-side weld bead geometry using weld pool surface characteristic parameters. J Intell Manuf 2013;25:1301–13. https://doi.org/10.1007/s10845-013-0731-4.
[194] Anawa EM, Olabi AG. Using Taguchi method to optimize welding pool of dissimilar laser-welded components. Opt Laser Technol 2008;40:379–88. https://doi.org/10.1016/j.optlastec.2007.07.001.
[195] Gao ZM, Shao XY, Jiang P, Wang CC, Zhou Q, Cao LC, et al. Multi-objective optimization of weld geometry in hybrid fiber laser-arc butt welding using kriging model and NSGA-II. Appl Phys A 2016;122:1–12. https://doi.org/10.1007/s00339-016-0144-2.
[196] Gao XD, Sun Y, Katayama S. Neural network of plume and spatter for monitoring high-power disk laser welding. Int J Precis Eng Manuf Technol 2014;1:293–8.

https://doi.org/10.1007/s40684-014-0035-y.
[197] Ai YW, Jiang P, Shao XY, Li P, Wang CC, Mi GY, et al. The prediction of the whole weld in fiber laser keyhole welding based on numerical simulation. Appl Therm Eng 2017;113:980–93. https://doi.org/10.1016/j.applthermaleng.2016.11.050.
[198] Gao XD, Mo L, Xiao ZL, Chen XH, Katayama S. Seam tracking based on Kalman filtering of micro-gap weld using magneto-optical image. Int J Adv Manuf Technol 2015;83:21–32. https://doi.org/10.1007/s00170-015-7560-x.
[199] Jia CB, Wu CS, Zhang YM. Sensing controlled pulse key-holing condition in plasma arc welding. Trans Nonferrous Met Soc China 2009;19:341–6. https://doi.org/10.1016/S1003-6326(08)60275-7.
[200] Mei LF, Chen GY, Jin XZ, Zhang Y, Wu Q. Research on laser welding of high-strength galvanized automobile steel sheets. Opt Lasers Eng 2009;47:1117–24. https://doi.org/10.1016/j.optlaseng.2009.06.016.
[201] Gao ZM, Jiang P, Mi GY, Cao LC, Liu W. Investigation on the weld bead profile transformation with the keyhole and molten pool dynamic behavior simulation in high power laser welding. Int J Heat Mass Transf 2018;116:1304–13. https://doi.org/10.1016/j.ijheatmasstransfer.2017.09.122.
[202] Pal S, Pal SK, Samantaray AK. Artificial neural network modeling of weld joint strength prediction of a pulsed metal inert gas welding process using arc signals. J Mater Process Technol 2008;202:464–74. https://doi.org/10.1016/j.jmatprotec.2007.09.039.
[203] Olabi AG, Casalino G, Benyounis KY, Hashmi MSJ. An ANN and Taguchi algorithms integrated approach to the optimization of CO2 laser welding. Adv Eng Softw 2006;37:643–8. https://doi.org/10.1016/j.advengsoft.2006.02.002.
[204] Lin HL, Chou CP. Modeling and optimization of Nd: YAG laser micro-weld process using Taguchi Method and a neural network. Int J Adv Manuf Technol 2008;37:513–22. https://doi.org/10.1007/s00170-007-0982-3.
[205] Badkar DS, Pandey KS, Buvanashekaran G. Parameter optimization of laser transformation hardening by using Taguchi method and utility concept. Int J Adv Manuf Technol 2010;52:1067–77. https://doi.org/10.1007/s00170-010-2787-z.
[206] Acherjee B, Kuar AS, Mitra S, Misra D. Application of grey-based Taguchi method for simultaneous optimization of multiple quality characteristics in laser transmission welding process of thermoplastics. Int J Adv Manuf Technol 2011;56:995–1006. https://doi.org/10.1007/s00170-011-3224-7.
[207] Ai YW, Wang JZ, Jiang P, Liu Y, Liu W. Parameters optimization and objective trend analysis for fiber laser keyhole welding based on Taguchi-FEA. Int J Adv Manuf Technol 2016;90:1419–32. https://doi.org/10.1007/s00170-016-9403-9.
[208] Ai YW, Shao XY, Jiang P, Li P, Liu Y, Yue C. Process modeling and parameter optimization using radial basis function neural network and genetic algorithm for laser welding of dissimilar materials. Appl Phys A 2015;121:555–69. https://doi.org/10.1007/s00339-015-9408-5.
[209] Cao LC, Yang Y, Jiang P, Zhou Q, Mi GY, Gao ZM, et al. Optimization of processing parameters of AISI 316L laser welding influenced by external magnetic field combining RBFNN and GA. Results Phys 2017;7:1329–38. https://doi.org/10.1016/j.rinp.2017.03.029.
[210] Rong YM, Zhang Z, Zhang GJ, Yue C, Gu YF, Huang Y, et al. Parameters optimization of laser brazing in crimping butt using Taguchi and BPNN-GA. Opt Lasers Eng 2015;67:94–104. https://doi.org/10.1016/j.optlaseng.2014.10.009.
[211] Yang Y, Cao LC, Wang CC, Zhou Q, Jiang P. Multi-objective process parameters optimization of hot-wire laser welding using ensemble of metamodels and NSGA-II. Robot Comput Integr Manuf 2018;53:141–52. https://doi.org/10.1016/j.rcim.2018.03.007.
[212] Sathiya P, Panneerselvam K, Jaleel MYA. Optimization of laser welding process parameters for super austenitic stainless steel using artificial neural networks and genetic algorithm. Materials & Design (1980-2015) 2012;36:490–8. https://doi.org/10.1016/j.matdes.2011.11.028.
[213] Liu S, Mi GY, Yan F, Wang CM, Jiang P. Correlation of high power laser welding parameters with real weld geometry and microstructure. Opt Laser Technol 2017;94:59–67. https://doi.org/10.1016/j.optlastec.2017.03.004.
[214] Lee S, Ahn S, Park C. Analysis of acoustic emission signals during laser spot welding of SS304 stainless steel. J Mater Eng Perform 2013;23:700–7. https://doi.org/10.1007/s11665-013-0791-9.
[215] Yu HW, Xu YL, Lv N, Chen HB, Chen SB. Arc spectral processing technique with its application to wire feed monitoring in Al–Mg alloy pulsed gas tungsten arc welding. J Mater Process Technol 2013;213:707–16. https://doi.org/10.1016/j.jmatprotec.2012.11.016.
[216] Zhang YX, Gao XD, Katayama S. Weld appearance prediction with BP neural network improved by genetic algorithm during disk laser welding. J Manuf Syst 2015;34:53–9. https://doi.org/10.1016/j.jmsy.2014.10.005.
[217] Zhang HJ, Wang FJ, Gao WG, Hou YY. Quality assessment for resistance spot welding based on binary image of electrode displacement signal and probabilistic neural network. Sci Technol Weld Join 2014;19:242–9. https://doi.org/10.1179/1362171813Y.0000000187.
[218] Luo M, Shin YC. Estimation of keyhole geometry and prediction of welding defects during laser welding based on a vision system and a radial basis function neural network. Int J Adv Manuf Technol 2015;81:263–76. https://doi.org/10.1007/s00170-015-7079-1.
[219] Wan XD, Wang YX, Zhao DW, Huang YA, Yin ZP. Weld quality monitoring research in small scale resistance spot welding by dynamic resistance and neural network. Measurement 2017;99:120–7. https://doi.org/10.1016/j.measurement.2016.12.010.
[220] Gunther J, Pilarski PM, Helfrich G, Shen H, Diepold K. Intelligent laser welding through representation, prediction, and control learning: an architecture with deep neural networks and reinforcement learning. Mechatronics 2016;34:1–11. https://doi.org/10.1016/j.mechatronics.2015.09.004.
[221] Regaard B, Kaierle S, Poprawe R. Seam-tracking for high precision laser welding applications—methods, restrictions and enhanced concepts. J Laser Appl 2009;21:183–95. https://doi.org/10.2351/1.3267476.
[222] Gao XD, Ding D, Bai TX, Katayama S. Weld-pool image centroid algorithm for seam-tracking vision model in arc-welding process. IET Image Process 2011;5:410. https://doi.org/10.1049/iet-ipr.2009.0231.
[223] Luo ZJ, Dai JS, Wang CY, Wang FL, Tian YL, Zhao MY. Predictive seam tracking with iteratively learned feedforward compensation for high-precision robotic laser welding. J Manuf Syst 2012;31:2–7. https://doi.org/10.1016/j.jmsy.2011.03.005.
[224] Gao XD, You DY, Katayama S. Infrared image recognition for seam tracking monitoring during fiber laser welding. Mechatronics 2012;22:370–80. https://doi.org/10.1016/j.mechatronics.2011.09.005.
[225] Ma HB, Wei SC, Sheng ZX, Lin T, Chen SB. Robot welding seam tracking method based on passive vision for thin plate closed-gap butt welding. Int J Adv Manuf Technol 2009;48:945–53. https://doi.org/10.1007/s00170-009-2349-4.
[226] Huang W, Kovacevic R. Development of a real-time laser-based machine vision system to monitor and control welding processes. Int J Adv Manuf Technol 2012;63:235–48. https://doi.org/10.1007/s00170-012-3902-0.
[227] Villan AF, Acevedo RG, Alvarez EA, Lopez AC, Garcia DF, Fernandez RU, et al. J.M. Garcia sanchez, low-cost system for weld tracking based on artificial vision. IEEE Trans Ind Appl 2011;47:1159–67. https://doi.org/10.1109/TIA.2011.2124432.
[228] Gu WP, Xiong ZY, Wan W. Autonomous seam acquisition and tracking system for multi-pass welding based on vision sensor. Int J Adv Manuf Technol 2013;69:451–60. https://doi.org/10.1007/s00170-013-5034-6.
[229] Nele L, Sarno E, Keshari A. An image acquisition system for real-time seam tracking. Int J Adv Manuf Technol 2013;69:2099–110. https://doi.org/10.1007/s00170-013-5167-7.
[230] Shi FH, Lin T, Chen SB. Efficient weld seam detection for robotic welding based on local image processing. Ind Robot Int J 2009;36:277–83. https://doi.org/10.1108/01439910910950559.
[231] Gao XD, You DY, Katayama S. Seam tracking monitoring based on adaptive kalman filter embedded elman neural network during high-power Fiber laser welding. Ieee Trans Ind Electron 2012;59:4315–25. https://doi.org/10.1109/TIE.2012.2193854.
[232] Gao XD, Zhong XG, You DY, Katayama S. Kalman filtering compensated by radial basis function neural network for seam tracking of laser welding. Ieee Trans Control Syst Technol 2013;21:1916–23. https://doi.org/10.1109/TCST.2012.2219861.
[233] Heber M, Lenz M, Rüther M, Bischof H, Fronthaler H, Croonen G. Weld seam tracking and panorama image generation for on-line quality assurance. Int J Adv Manuf Technol 2012;65:1371–82. https://doi.org/10.1007/s00170-012-4263-4.
[234] Mirapeix J, Ruiz-Lombera R, Valdiande JJ, Rodriguez-Cobo L, Anabitarte F, Cobo A. Defect detection with CCD-spectrometer and photodiode-based arc-welding monitoring systems. J Mater Process Technol 2011;211:2132–9. https://doi.org/10.1016/j.jmatprotec.2011.07.011.
[235] Chu HH, Wang ZY. A vision-based system for post-welding quality measurement and defect detection. Int J Adv Manuf Technol 2016;86:3007–14. https://doi.org/10.1007/s00170-015-8334-1.
[236] Wang T, Chen JQ, Gao XD, Qin YX. Real-time monitoring for disk laser welding based on feature selection and SVM. Appl Sci 2017;7:884. https://doi.org/10.3390/app7090884.
[237] Levesque D, Dubourg L, Blouin A. Laser ultrasonics for defect detection and residual stress measurement of friction stir welds. Nondestruct Test Eval 2011;26:319–33. https://doi.org/10.1080/10589759.2011.573551.
[238] Ai YW, Jiang P, Wang CC, Mi GY, Geng SN, Liu W, et al. Investigation of the humping formation in the high power and high speed laser welding. Opt Lasers Eng 2018;107:102–11. https://doi.org/10.1016/j.optlaseng.2018.03.010.
[239] Gao XD, Ma N, Du LJ. Magneto-optical imaging characteristics of weld defects under alternating magnetic field excitation. Opt Express 2018;26:9972–83. https://doi.org/10.1364/OE.26.009972.
[240] Nicolosi L, Abt F, Blug A, Heider A, Tetzlaff R, Höfler H. A novel spatter detection algorithm based on typical cellular neural network operations for laser beam welding processes. Meas Sci Technol 2012;23:015401https://doi.org/10.1088/0957-0233/23/1/015401.
[241] You DY, Gao XD, Katayama S. Detection of imperfection formation in disk laser welding using multiple on-line measurements. J Mater Process Technol 2015;219:209–20. https://doi.org/10.1016/j.jmatprotec.2014.12.025.
[242] You DY, Gao XD, Katayama S. Multisensor fusion system for monitoring high-power disk laser welding using support vector machine. IEEE Trans Industr Inform 2014;10:1285–95. https://doi.org/10.1109/TII.2014.2309482.
[243] Rodil SS, Gomez RA, Bernardez JM, Rodríguez F, Miguel LJ, Peran JR. Laser welding defects detection in automotive industry based on radiation and spectroscopical measurements. Int J Adv Manuf Technol 2009;49:133–45. https://doi.org/10.1007/s00170-009-2395-y.
[244] Sumesh A, Rameshkumar K, Mohandas K, Babu RS. Use of machine learning algorithms for weld quality monitoring using acoustic signature. Procedia Comput Sci 2015;50:316–22. https://doi.org/10.1016/j.procs.2015.04.042.
[245] Zhang ZF, Yu HW, Lv N, Chen SB. Real-time defect detection in pulsed GTAW of Al alloys through on-line spectroscopy. J Mater Process Technol 2013;213:1146–56. https://doi.org/10.1016/j.jmatprotec.2013.01.012.
[246] Zhang ZF, Kannatey-Asibu E, Chen SB, Huang YM, Xu YL. Online defect detection of Al alloy in arc welding based on feature extraction of arc spectroscopy signal. Int J Adv Manuf Technol 2015;79:2067–77. https://doi.org/10.1007/s00170-015-6966-9.
[247] Gao XD, Xie YL, Du LL, Chen ZQ, Song YW, Gao PP. Detection of weld cracks using magneto-optical imaging. 2018 IEEE 14th International Conference on

Automation Science and Engineering (CASE) 2018:559–64.
[248] Flint TF, Francis JA, Smith MC, Balakrishnan J. Extension of the double-ellipsoidal heat source model to narrow-groove and keyhole weld configurations. J Mater Process Technol 2017;246:123–35. https://doi.org/10.1016/j.jmatprotec.2017.02.002.
[249] Bachmann M, Avilov V, Gumenyuk A, Rethmeier M. Numerical simulation of full-penetration laser beam welding of thick aluminium plates with inductive support. J Phys D Appl Phys 2012;45:035201https://doi.org/10.1088/0022-3727/45/3/035201.
[250] Svenungsson J, Choquet I, Kaplan AFH. Laser welding process – a review of keyhole welding modelling. Phys Procedia 2015;78:182–91. https://doi.org/10.1016/j.phpro.2015.11.042.
[251] Moos S, Vezzetti E. Resistance spot welding process simulation for variational analysis on compliant assemblies. J Manuf Syst 2015;37:44–71. https://doi.org/10.1016/j.jmsy.2015.09.006.
[252] Rao ZH, Liao SM, Tsai HL. Modelling of hybrid laser–GMA welding: review and challenges. Sci Technol Weld Join 2013;16:300–5. https://doi.org/10.1179/1362171811Y.0000000022.
[253] Volpp J, Vollertsen F. Keyhole stability during laser welding—part I: modeling and evaluation. Prod Eng 2016;10:443–57. https://doi.org/10.1007/s11740-016-0694-3.
[254] Geiger M, Leitz KH, Koch H, Otto A. A 3D transient model of keyhole and melt pool dynamics in laser beam welding applied to the joining of zinc coated sheets. Prod Eng 2009;3:127–36. https://doi.org/10.1007/s11740-008-0148-7.
[255] Abderrazak K, Bannour S, Mhiri H, Lepalec G, Autric M. Numerical and experimental study of molten pool formation during continuous laser welding of AZ91 magnesium alloy. Comput Mater Sci 2009;44:858–66. https://doi.org/10.1016/j.commatsci.2008.06.002.
[256] Zhao SS, Yu G, He XL, Zhang YJ, Ning WJ. Numerical simulation and experimental investigation of laser overlap welding of Ti6Al4V and 42CrMo. J Mater Process Technol 2011;211:530–7. https://doi.org/10.1016/j.jmatprotec.2010.11.007.
[257] Kazemi K, Goldak JA. Numerical simulation of laser full penetration welding. Comput Mater Sci 2009;44:841–9. https://doi.org/10.1016/j.commatsci.2008.01.002.
[258] Pang SY, Chen WD, Wang W. A quantitative model of keyhole instability induced porosity in laser welding of titanium alloy. Metall Mater Trans A 2014;45:2808–18. https://doi.org/10.1007/s11661-014-2231-3.
[259] Pang SY, Shao XY, Li W, Chen X, Gong SL. Dynamic characteristics and mechanisms of compressible metallic vapor plume behaviors in transient keyhole during deep penetration fiber laser welding. Appl Phys A 2016;122. https://doi.org/10.1007/s00339-016-0230-5.
[260] Zhang YX, Han SW, Cheon J, Na SJ, Gao XD. Effect of joint gap on bead formation in laser butt welding of stainless steel. J Mater Process Technol 2017;249:274–84. https://doi.org/10.1016/j.jmatprotec.2017.05.040.
[261] Wu SJ, Gao HM, Zhang W, Zhang YM. Real-time estimation of weld penetration using weld pool surface based calibration. IEEE Industrial Electronics Society. IEEE; 2016. p. 294–9.
[262] Farrokhi F, Endelt B, Kristiansen M. A numerical model for full and partial penetration hybrid laser welding of thick-section steels. Opt Laser Technol 2018;111:671–86. https://doi.org/10.1016/j.optlastec.2018.08.059.
[263] Frostevarg J. Factors affecting weld root morphology in laser keyhole welding. Opt Lasers Eng 2018;101:89–98. https://doi.org/10.1016/j.optlaseng.2017.10.005.
[264] Pan QL, Mizutani M, Kawahito Y, Katayama S. High power disk laser-metal active gas arc hybrid welding of thick high tensile strength steel plates. J Laser Appl 2016;28:012004https://doi.org/10.2351/1.4934939.
[265] Li XC, Farson D, Richardson R. Weld penetration control system design and testing. J Manuf Syst 2001;19:383–92. https://doi.org/10.1016/S0278-6125(01)80010-8.
[266] Abt F, Heider A, Weber R, Graf T, Blug A, Carl D, et al. Camera based closed loop control for partial penetration welding of overlap joints. Phys Procedia 2011;12:730–8. https://doi.org/10.1016/j.phpro.2011.03.091.
[267] Purtonen T, Kalliosaari A, Salminen A. Monitoring and adaptive control of laser processes. Phys Procedia 2014;56:1218–31. https://doi.org/10.1016/j.phpro.2014.08.038.
[268] Liu YK, Zhang YM. Iterative local ANFIS-Based human welder intelligence modeling and control in pipe GTAW process: a data-driven approach. Ieee/asme Trans Mechatron 2015;20:1079–88. https://doi.org/10.1109/TMECH.2014.2363050.
[269] Stehr T, Hermsdorf J, Henning T, Kling R. Closed loop control for laser micro spot welding using fast pyrometer systems. Phys Procedia 2010;5:465–71. https://doi.org/10.1016/j.phpro.2010.08.074.
[270] Hofman JT, Pathiraj B, van Dijk J, de Lange DF, Meijer J. A camera based feedback control strategy for the laser cladding process. J Mater Process Technol 2012;212:2455–62. https://doi.org/10.1016/j.jmatprotec.2012.06.027.
[271] Craeghs T, Bechmann F, Berumen S, Kruth JP. Feedback control of Layerwise Laser melting using optical sensors. Phys Procedia 2010;5:505–14. https://doi.org/10.1016/j.phpro.2010.08.078.
[272] Mrna L, Sarbort M, Rerucha S, Jedlicka P. Feedback control of laser welding based on frequency analysis of light emissions and adaptive beam shaping. Phys Procedia 2012;39:784–91. https://doi.org/10.1016/j.phpro.2012.10.101.
[273] Sibillano T, Rizzi D, Mezzapesa FP, Lugara PM, Konuk AR, Aarts R, et al. Closed loop control of penetration depth during CO(2) laser lap welding processes. Sensors (Basel) 2012;12:11077–90. https://doi.org/10.3390/s120811077.
[274] Li XR, Zhang YM, Kvidahl L. Penetration depth monitoring and control in submerged arc welding. Weld J 92. 2013. p. S48–56.
[275] Liu YK, Zhang YM. Model-based predictive control of weld penetration in gas tungsten arc welding. Ieee Trans Control Syst Technol 2014;22:955–66. https://doi.org/10.1109/TCST.2013.2266662.
[276] Liu YK, Zhang WJ, Zhang YM. Dynamic neuro-fuzzy-Based human intelligence modeling and control in GTAW. Ieee Trans Autom Sci Eng 2015;12:324–35. https://doi.org/10.1109/TASE.2013.2279157.
[277] Liu YK, Zhang YM. Toward welding robot with human knowledge: a remotely-controlled approach. Ieee Trans Autom Sci Eng 2015;12:769–74. https://doi.org/10.1109/TASE.2014.2359006.
[278] Lee J, Kao HA, Yang S. Service innovation and smart analytics for industry 4.0 and big data environment. Procedia Cirp 2014;16:3–8. https://doi.org/10.1016/j.procir.2014.02.001.
[279] Mahrle A, Borkmann M, Beyer E, Leyens C, Hustedt M, Hennigs C, et al. Efficient air flow control for remote laser beam welding. J Laser Appl 2018;30:032413.
[280] Negel JP, Abt F, Blazquez-Sanchez D, Austerschulte A, Hafner M, et al. Controlling the thermally induced focal shift in laser processing heads. Conference on High Power Laser Materials Processing - Lasers, Beam Delivery, Diagnostics, and Applications 2012;8239:823911https://doi.org/10.1117/12.906634.
[283] Nguyen G, Dlugolinsky S, Bobak M, Tran V, Garcia AL, Heredia I, et al. Machine Learning and Deep Learning frameworks and libraries for large-scale data mining: a survey. Artif Intell Rev 2019;52:77–124. https://doi.org/10.1007/s10462-018-09679-z.
[284] Ruan XF, Jiang P, Zhou Q, Hu JX, Shu LS. Variablefidelity probability of improvementmethod for efficient global optimization of expensive black-box problems. Struct Multidiscip O 2020:1–32. https://doi.org/10.1007/s00158-020-02646-9.